Final Report on NASA contract NAGW-3318

Assessing the Geomorphic Evolution and Hydrographic Changes Induced by Winter Storms along the Louisiana Coast

for the period of

1 April 1993 to 30 September 1997

submitted by

W Paul Menzel

Christopher C. Moeller

Cooperative Institute for Meteorological Satellite Studies (CIMSS)

University of Wisconsin

1225 West Dayton Street

Madison, Wisconsin 53706

and

Oscar K. Huh

Harry H. Roberts

Coastal Studies Institute (CSI)

Louisiana State University

308 Howe-Russell Geoscience Complex

Baton Rouge, Louisiana 70803

February 1998

I. INTRODUCTION

The influence that cold front passages have on Louisiana coastal environments, including land loss and land building processes, has been the primary topic of this multidisciplinary research. This research has combined meteorological, remote sensing, and coastal expertise from the University of Wisconsin (UW) and Louisiana State University (LSU). Analyzed data sets include remotely sensed radiometric data (AVHRR on NOAA-12,13,14, Multispectral Atmospheric Mapping Sensor (MAMS) and MODIS Airborne Simulator (MAS) on NASA ER-2), U.S. Army Corps of Engineers (USACE) water level data, water quality data from the Coastal Studies Institute (CSI) at LSU, USACE river discharge data, National Weather Service (NWS) and CSI wind *in situ* measurements, geomorphic measurements from aerial photography (NASA ER-2 and Learjet), and CSI ground based sediment burial pipes (for monitoring topographic change along the Louisiana coast) and sediment cores. The work reported here-in is a continuation of an initial investigation into coastal Louisiana landform modification by cold front systems. That initial effort demonstrated the importance of cold front winds in the Atchafalaya Bay sediment plume distribution (Moeller et al. 1993), documented the sediment transport and deposition process of the western Louisiana coast (Huh et al. 1991) and developed tools (e.g. water types identification, suspended solids estimation) from multispectral radiometric data for application to the current study. This study has extended that work, developing a Geomorphic Impact Index (GI^2) for relating atmospheric forcing to coastal response and new tools to measure water motion and sediment transport.

Cold fronts impact coastal regions through their associated wind, temperature, and pressure patterns, causing redistribution of suspended sediment (SSC), water level fluctuation, wave action, and by affecting water temperatures and moisture content of fresh shoreline sediment deposits (Roberts et al. 1987). This study has contributed analyses of coastal circulation, suspended sediment transport, water types, and

geomorphic response to wind system forcing by cold front passages. Primary findings of this study are:

1. **Geomorphic impact on Louisiana's muddy coast region by cold front passages can be parameterized using wind energy in combination with water level. In particular, only during high water level events is the cold front wind energy effective in imparting geomorphic impact. This finding is the basis of the Geomorphic Impact Index (GI^2), which can be used to assess seasonal to interannual impact on coastal landforms.**
2. **Estimates of water motion and sediment transport indicate large short term variation of nearshore circulation and mass transport, intermittently feeding and starving coastal estuaries and nearshore waters with land-building material. The implications of this finding for maintaining coastal marine ecosystems are not yet fully understood. This finding was made possible by the use of the NASA ER-2 research aircraft, which had the capability to collect high spatial (100m or better) and temporal (1-2 hours) resolution data.**
3. **A method of multispectral coastal water type analysis has been developed using a combination of water surface temperature and visible/near IR subsurface reflectance in a postfrontal scatter plot analysis. Remote sensing measurements made by MAMS (100m resolution) and MAS (50m resolution) on the ER-2 show five distinguishable water types including river water, estuarine water, inner shelf water, marsh drainage, and soil water drainage (Huh et al. 1996) in the Atchafalaya Bay area of Louisiana. The water types illustrate coastal processes such as marsh drainage, soil de-watering, and estuarine-saltwater exchange.**
4. **Frequent, synoptic scale (but lower energy) cold front systems appear to be more important than the infrequent, generally localized (but powerful) tropical systems. However, longer periods of record are necessary to fully assess impacts of cold fronts and tropical systems.**

Table of Contents

Because of the difficulty of gathering surface data in inaccessible coastal environments, this study was designed to apply remote sensing as a primary source of information for coastal research. This project thus served as a testing ground for the informational content of high resolution remote sensing measurements in a coastal environment. The understandings gained from this effort will benefit the application of multispectral observations from the MODIS instrument (estimated launch in 1998).

II. RESEARCH ACCOMPLISHMENTS

A. Data Collection and Observations

1. Remote Sensing and Ancillary Data Collection

MAMS and, starting in 1994, MAS were flown on NASA's ER-2 aircraft over the Louisiana coast beginning with the cold front season of 1987-88. A detailed description of the MAMS instrument is available in Jedlovec et al. (1989); details on MAS can be found in King et al. (1996). A list of Louisiana coast flights through the end of this grant is shown in Table 1. The ER-2 flights comprise an eight year, high spatial resolution remote sensing data record of the Louisiana coastal region. The data flights were planned to optimize clear sky data collection over the coastal zone. During most flights, CSI boat teams collected water quality measurements in the Atchafalaya Bay region. *In situ* measurements included suspended sediment concentration (SSC), sea surface temperature (SST), secchi disk depth (SDD), and CTD measurements. The MAMS and MAS data sets have been split into straight line flight track segments, navigated, and archived on tape for future use.

In addition, the NASA ER-2 aircraft collected 5 and 10 meter resolution false color infrared aerial photography data during most flights. These data were used to monitor small scale changes in geomorphology, and also served as a verification tool for the MAMS and MAS observations.

AVHRR imagery from the NOAA series polar orbiting satellites was used to maintain a daily surveillance of the turbid waters of the Atchafalaya Bay/Chenier Plain coastal sedimentary system. Both sea surface temperature and suspended sediment calculations were made from the AVHRR 1 km imagery at the LSU Earth Scan

Table 1. - MAMS/MAS Louisiana Coast Flight Summary

DATE[1]	COVERAGE[2]	*in situ*	COMMENTS
01/27/88	Type 1		postfrontal, low water
08/26/88	Type 1		summer; thin cirrus
11/02/88	Type 1	X	cirrus
03/30/89	Type 1		prefrontal; SW wind high water
04/01/89	Type 1	X	postfrontal; NE wind; FROPA pair w/Mar30
04/06/89	Type 2		triple overpass; high water transition to prefrontal
12/13/89	Type 1	*	postfrontal; low water
04/15/90	Type 2		triple overpass; postfrontal; high water
04/16/90	Type 1		transition to prefrontal; high water
12/04/90	Type 2	X	postfrontal; low water
12/05/90	Type 1	X	postfrontal; light winds consecutive w/Dec 4
03/30/91	Type 2		triple overpass; postfrontal; cloud streets
04/01/91	Type 1		postfrontal
11/24/91	Type 1		MAS flyby
12/11/92	Type 1	X	postfrontal; some cirrus
02/02/94	Type 1	X	MAS; transition to prefrontal
02/14/94	Type 2	X	MAS; triple pass; postfrontal
02/17/94	Type 1	X	MAS; postfrontal; stratus; high water
01/08/95	Type 1	X	MAS; postfrontal; high water
01/24/95	Type 2	X	MAS; postfrontal; triple pass
04/09/96	Type 2	X	MAS; postfrontal; triple pass high water

Notes:
1. For flights before 1995, 12 channel digitizer used (7 channels @ 8 bit precision, 4 channels @ 10 bit precision, 1 channel for extra bit bucket). Beginning in Jan 1995, 50 channel digitizer used.(50 channels @ 12 bit)
2. Type 1 flights cover full Louisiana coastline in 4 flight lines. Type 2 flights use racetrack pattern to repeatedly overfly selected sites (typically the Atchafalaya Bay region of the Louisiana coast).

* Boat ramp water level too low to launch boat.

Laboratory, a multisatellite ground station. A suspended sediment algorithm (Stumpf, 1992) using Rayleigh corrected channel 1 minus channel 2 was used to map the distribution of turbid waters. The algorithm has been calibrated against water samples collected by helicopter (Walker et al. 1996). This allowed detection of the size and orientation of river/estuarine discharges, and flow paths of the suspended sediments throughout the region. The AVHRR imagery was also used to direct field activities for surface *in situ* sampling.

In addition to remote sensing and boat *in situ* data sets, the following data sets were collected:

1) National Weather Service surface wind data for the years 1990-1997 at Lake Charles and New Orleans, LA.
2) Atchafalaya River discharge (daily) and sediment load (bi-weekly) for 1980-1997.
3) Water level data at the Amerada Hess platform near Eugene Island, 1987-1997.
4) Special surface wind (1995-1997) and tidal gauge (July 1995) data sets at instrumented Fina #13 platform in nearshore Gulf of Mexico for 1995-1997.
5) Deployment of topographic sediment monitoring pipes and seasonal measurements of topographic change (1994-1997).

These data were applied primarily to the formulation and analysis of the Geomorphic Impact Index, which relates meteorological forcing of cold fronts to coastal geomorphology.

2. Suspended Sediment Monitoring and Transport

Suspended sediment distribution and transport were monitored using MAMS and MAS atmospherically corrected visible/near IR reflectances, calibrated to SSC using *in situ* measurements (from boat teams deployed by CSI during ER-2 flights). Atmospheric correction was based on work by Gordon et al. (1983), Guzzi and Zibordi (1987), and Gumley et al. (1990). Repeat coverage MAS and MAMS SSC maps proved useful for

estimating water motion and sediment transport in the turbid Atchafalaya Bay region (Moeller et al. 1996). Maps of water velocity and sediment transport demonstrate significant small scale variability and show that velocity and sediment transport are not highly correlated (Figure 1). Transport of suspended material is central to both terrestrial and subaqueous geomorphic evolution. Effects of sediment deposition on the delicate estuarine ecosystem are not well understood at this time but are of great economic interest (e.g. destruction of oyster beds, freshwater versus brackish water domination).

3. Coastal Water Types Detection

Coastal waters in plan view are generally a mosaic of waters of different temperatures and turbidities (Huh et al. 1996). Water types are particularly variant in regions such as the Louisiana coast where the Mississippi River and estuarine discharges create a range of suspended sediment concentrations (0-1200mg/l). Experimentation with MAMS imagery resulted in the critical observation that there is an inverse correlation between the visible/near infrared reflectances and the water surface temperature (Moeller et al. 1989). This correlation made possible a temperature/turbidity analysis similar to the classical temperature/salinity analysis essential to identifying oceanic water types. Water type analysis has turned out to be a useful tool in the study of coastal circulation and water type formation processes, particularly after a cold front passage.

B. Geomorphic Developments in the S.W. Louisiana Coastal Zone

Investigation into relationships between external influences (e.g. cold front wind systems, water level variation, etc.) and geomorphology of the Louisiana coast were a primary topic of the project. Specifically, it has been observed that the easternmost portion of the Louisiana Chenier Plain has changed within the last decade from an erosional to a progradational sedimentary regime. The progradational/accretional deposits are sheets of fine grained sediment. Geological studies of these washover deposits implicate the

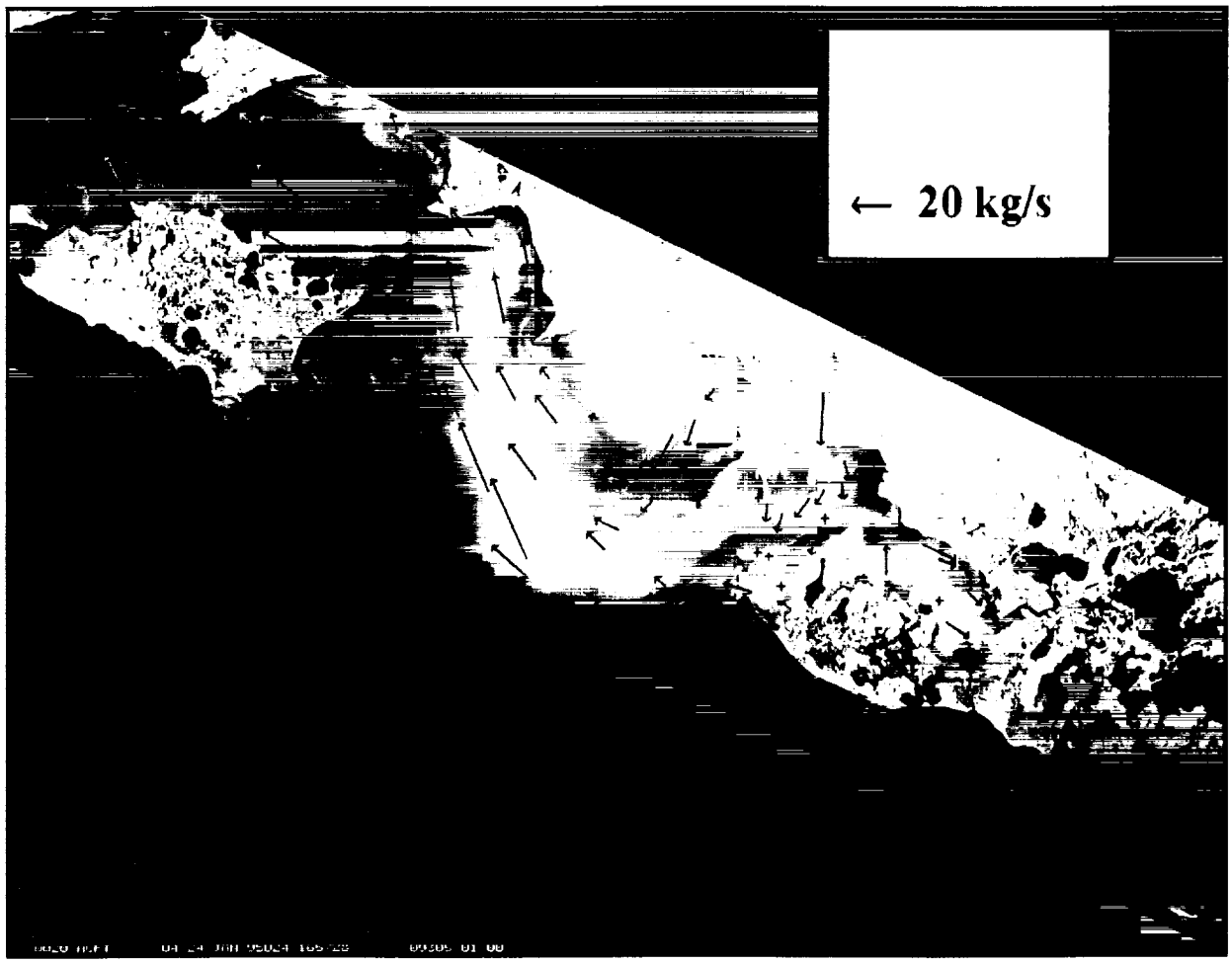

Figure 1. MAS near infrared imagery of Atchafalaya Bay region of the central Louisiana coast on 24 January 1995. Image is remapped from aircraft projection to Mercator projection. On 24 January, the ER-2 flew three consecutive overpasses of the Atchafalaya Bay in a two hour period. The images were remapped to Mercator projection, animated, and targets were selected and tracked from image to image providing the water motion (green arrows) analysis shown. Sediment transport estimates (red arrows) were produced by combining water motion vectors with MAS SSC map. Water motion errors due to "jitter" in remapped imagery are estimated at about 10-20% of vector speed (based on tracking land jitter). MAS SSC regression uncertainty of 38mg/l is also about 10-20% error.

southerly winds and storm surges of cold fronts and other storms as primary forcing mechanisms for coastal accretion and progradation. The approach chosen was to measure the changes in the coastal deposits at the particularly active sites of western Louisiana and relate those measurements to the external forcing. The ultimate goal of this effort was to develop a Geomorphic Impact Index (GI^2), which amalgamates the external influences into a measure of actual or potential coastal landform change.

1. Geomorphological Surveys and Measurements

Measurements of lateral accretion, vertical accretion, and erosion along the western Louisiana coast were made using aerial photography (NASA ER-2 and Learjet) and arrays of ground based sediment burial pipes. Aerial photography (1987-1997) was used to estimate lateral changes both shore normal and shore parallel; an array of sediment burial pipes (1994-1997) were used to monitor the vertical accretion. The sediment burial pipes remain in place as useful reference points from which to monitor geomorphic change in years to come.

Land accretion and erosion in the aerial photography was measured manually using identifiable landmarks in the photography at several sites along the western Louisiana coast. Of primary interest is the muddy prograding coastal region westward (and downdrift) of the sediment rich Atchafalaya River mouth and Bay. Identifiable landmarks (canals, structures, etc.) along this muddy coast were used as "anchor" sites to measure mud area over a 10 year period of aerial photographic surveys (some 40 different dates, from 1987-1997). Active erosional sites to the west and east of the muddy coast were also monitored.

Sediment burial pipes (galvanized iron) were installed at active sites of geomorphic change along the muddy coast region in November 1994. The pipes were forced some 3 to 5 meters into the recent mud deposit, hitting a firm, nearly impenetrable substrate (probably the Pleistocene surface, i.e. 6cm to refusal) to assure vertical and lateral

stability. Measurements were made from clamps on the pipes to the surface of sedimentation.

2. Sources of Mud and the Deposition Cycle

The material deposited on the muddy coast originates in the Atchafalaya River outflow. This is evidenced by remote sensing imagery (AVHRR, MAS, and MAMS) which shows the Atchafalaya River sediment plume extending downdrift from the Atchafalaya Bay to the muddy western Louisiana coast. Additional evidence for the sediment source is given by the huge quantities of water hyacinth strewn along the muddy coast; the Atchafalaya River is virtually the sole source of these plants. Much of the subaqueous bottom from the Atchafalaya Bay to the muddy coast is layered with mud deposits of varying viscosity. In the regions of greatest shoreface deposition, these massive mud deposits have a consistency of heavy cream or "yogurt" and are referred to as fluid mud. Sediment cores offshore of the muddy coast typically show several centimeters of a light yellowish brown mud overlying a dark gray to black mud of a sub-bottom reducing environment. The light yellowish brown sediment is the newly deposited fine grained silts and clays that are characteristic of suspended sediment in the Atchafalaya River sediment plume. The dark gray to black sediment from beneath the sedimentary surface of the inner shelf is episodically exhumed by erosive wave action, creating a black "surf zone". During strong cold fronts, which supply the energy for resuspension and deposition events, both fluid mud and the suspended sediment material in the plume are sources of deposition material. In the prefrontal phase, onshore winds drive up nearshore water levels. If high water levels are attained, the resuspended fluid mud and suspended fine grain sediments are washed over the muddy coast and deposited. In the postfrontal phase, the cold, dry offshore winds set down the nearshore water levels, stranding and dewatering the mud deposits. In the quiescent interludes between strong storms, the sediment plume acts to replenish fluid mud by sediments precipitating from the plume.

3. Geomorphic Impact Index

The Geomorphic Impact Index (GI^2), which relates atmospheric forcing to coastal geomorphology response, was tested using three primary predictors: wind energy, water level, and the presence of deposition material (i.e. suspended sediments). The model tests the theory that southerly wind energy, in the presence of suspended sediments, translates into onshore sediment transport along the Chenier Plain muddy coast of western Louisiana. The combination of large wind energy, high water levels, and much available fine grained sediment is the most potent condition for coastal geomorphic accretion. This set of conditions often occurs in the springtime when southerly winds ahead of cold front passages (often stalling over land) appear to be maximized and spring river floods supply vast quantities of sediment. Wind energy was monitored using surface observations from the Lake Charles, LA NWS station. Optimally, surface winds should be monitored in the nearshore waters just offshore; however, the NWS data represented the best continuous long term surface wind data set available within close proximity to the coast. Water level was represented by the Amerada Hess USACE station in the Atchafalaya Bay, about 80 km east of the Chenier Plain study site. Sediment availability was monitored using the Atchafalaya River stream flow volume data provided by the USACE. It is noteworthy that the Atchafalaya River sediment plume/mud stream does not consistently follow the prevailing westward drift of the coastal current, but is variously wind driven to the east, south or west (as shown by MAMS, MAS, and AVHRR imagery). This phenomenon is not accounted for in the use of streamflow data to estimate the presence of depositional material along the muddy coast. However, findings of this work indicate that the Chenier Plain muddy coast is not sediment starved.

The investigation relied upon regression techniques. Aerial photography observations (2/15/91, 2/28/92, 4/9/93, 2/2/94, 1/8/95, 4/08/96, and 6/3/97) were used to manually estimate incremental mud area (mud accumulation/loss on the shoreface from year to year) for the muddy coast region of the Chenier Plain. These geomorphic

measurements were considered to be accurate to within about 10-20%. Wind energy data were summed between the dates of the geomorphic measurements and separated into water level bins (-0.5' to 0.0', 0.0' to 0.5', 0.5' to 1.0', 1.5' to 2.0', >2.0'). Importantly, it was found that wind energy was most correlated to incremental mud area on the Chenier Plain when water levels at Amerada Hess were highest (greater than 2 feet). This implies that water levels must be near or exceed the elevation of the Chenier Plain muddy shoreface to deposit new mud onshore. A separate regression of river discharge and incremental mud area showed no identifiable relationship, indicating that fluid mud is persistently present along the Chenier Plain (although its replenishment by westward drift of the Atchafalaya sediment plume is intermittent).

The GI^2 expression used is

$$GI^2(n) = -319500 + 28.06\sum_{n-1}^{n} WE(2)$$

where $GI^2(n)$ is the Geomorphic Impact Index for date number n. WE(2) is the summed Wind Energy when water levels exceed 2 feet. This expression explains 64% of the variance in the incremental mud area; the relationship is graphically depicted in Figure 2. With the exception of the 1993 sample, the model trends quite well with the observations. In spite of reviewing available data, no explanation has yet been found for the 1993 anomaly. Overall, these results are promising in linking the atmospheric forcing to sediment dynamics in the coastal zone; however, they are applicable only to the muddy Chenier Plain coast of western Louisiana and are based on a limited, though carefully drawn, sample (1 data point per year for seven years).

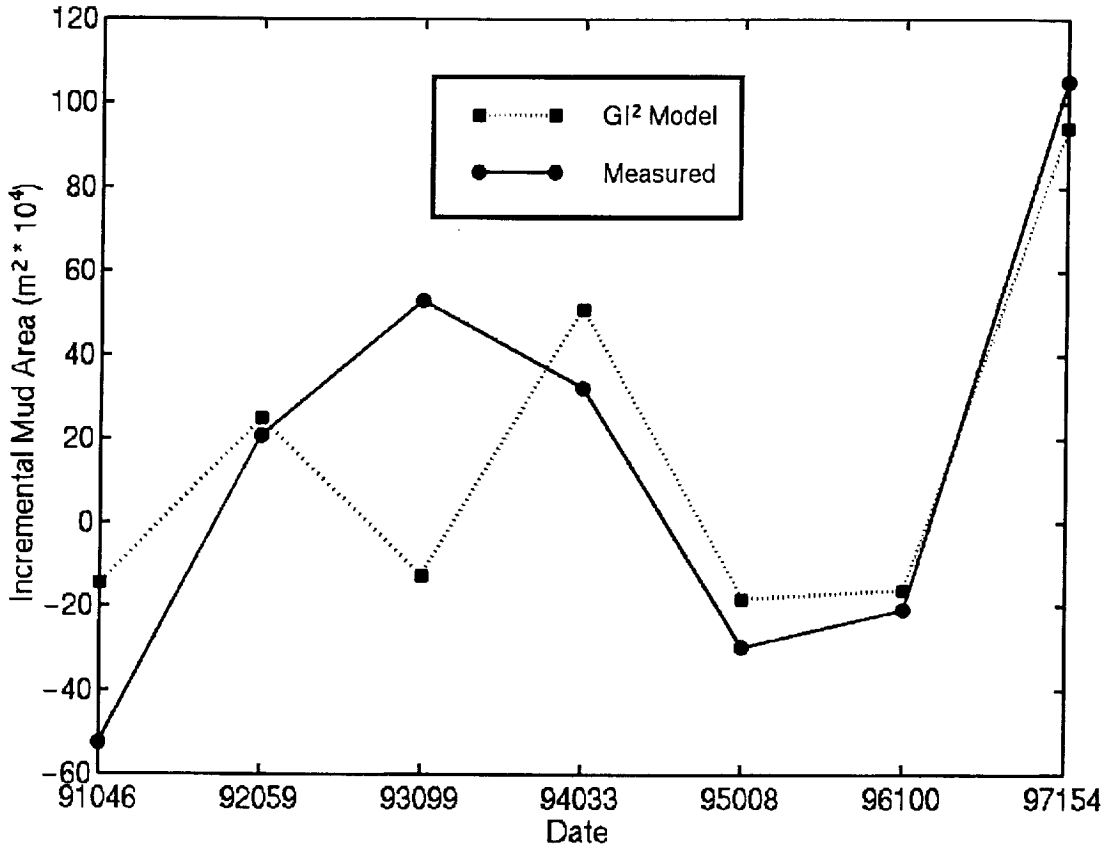

Figure 2. Geomorphic change of the muddy coast portion of the Chenier Plain of western Louisiana, observed and predicted by the Geomorphic Impact Index (GI^2). Observed measurements taken from aerial photography; GI^2 is based on surface wind energy during high water level events along the Louisiana coast. The physical interpretation of the GI^2 is that wind energy causes resuspension and shoreward transport of suspended sediments which, if water levels are high enough, results in shoreface deposition. Incremental Mud Area is the change in mud area along the Chenier Plain from one aerial photography date to the next. The GI^2 model traces the observations quite well, particularly from 1994 through 1997. No explanation was found for the anomalous behavior of 1993, a year when mud growth was observed, but little wind energy was present to drive suspended sediments onshore.

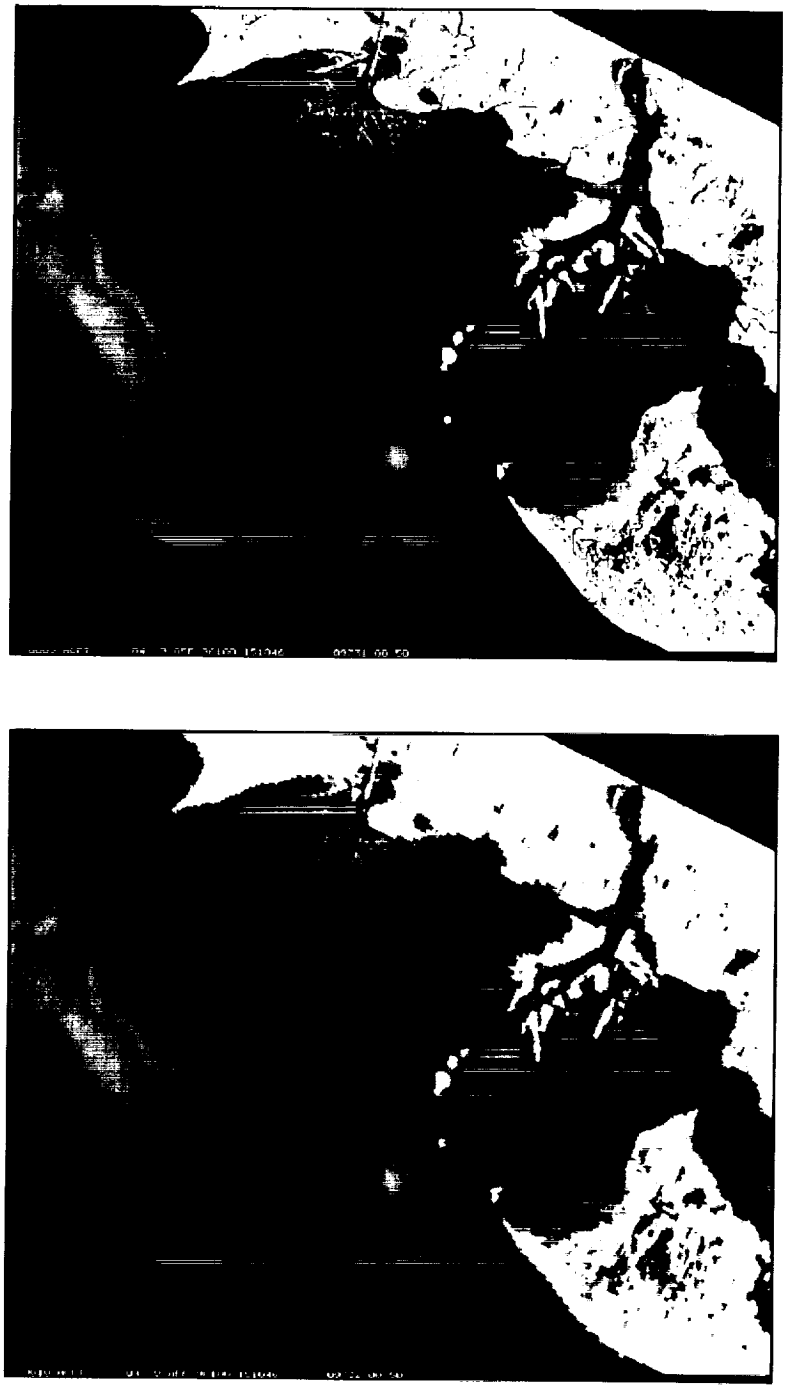

Figure 3. MAS near IR imagery of Atchafalaya Bay, Louisiana at full (50 meter) resolution (top) and at simulated MODIS 250 meter resolution. Most turbidity features in the bay will be detectable with MODIS data. Blurring of narrow inland waterways is significant. Imagery taken from April 9 1996 ER-2 overflight of Louisiana coast.

C. Implications for Applying MODIS data to Coastal Studies

MODIS will be launched in mid-1998 on board the AM-1 platform. In its polar orbit, MODIS will overfly the Louisiana Gulf coast region twice daily. MODIS contains two reflectance channels at 250m spatial resolution, a red channel and a near IR channel. These channels will be able to depict fine scale features in turbid water of the Louisiana coastal zone (Figure 3) and will be very useful for SSC estimates, coastal circulation information, and water types analysis (although the thermal band is available at only 1km resolution). After the launch of PM-1 in 2000, it will be possible to identify water motions using the 250m bands from AM-1 and PM-1 together.

D. Remaining Questions

A number of questions remain concerning the response of sediment distribution, transport, and deposition to atmospheric forcing and the resultant impact on the Louisiana coastal environment. A few of these are:

1) Can cold fronts be classified by their associated processes so that geomorphic response can be predicted by knowing the cold front type?

2) What are the details of the geomorphic/sedimentological processes of coastal change set in motion by cold fronts and tropical systems?

3) Do different aspects/phases of the cold front system dictate the response of the various types of coastal environments (e.g. estuaries, marshes, deltas, etc.)?

4) What are the nearshore oceanic responses to cold front events (circulation change, water level change, wave activity)? Are individual strong cold fronts more important than multiple weak fronts to these responses?

5) What are the Geomorphic/Sedimentological impacts on the inner shelf (subaqueous mud redistribution, replenishing sediment supply, sedimentary structure) by cold fronts? Are critical levels of storm strength required before important impact occurs?

6) What are the marine ecological responses to sediment redistribution, transport and deposition (nursery environments, oyster beds, breeding grounds)?

7) What are the consequences of Earth-Atmosphere System Global Change for the creation, maintenance, and vitality of fragile coastal ecosystems (fewer and stronger cold fronts, increased tropical activity, rising sea level, increased river discharge)?

III. LIST OF PAPERS RESULTING FROM NAGW-3318

Huh, O. K., C. C. Moeller, W. P. Menzel, and H. H. Roberts: Process and change detection in coastal environments with multispectral scanners and aerial photography. Second International Airborne Remote Sensing Conference and Exhibition, Vol II, June 24-27, 1996, San Francisco, CA, ERIM, 689-701, 1996.

Huh, O. K., C. C. Moeller, W. P. Menzel, L. J. Rouse Jr., and H. H. Roberts, "Remote sensing of turbid coastal and estuarine water: a method of multispectral water-type analysis". *J. of Coastal Research*, Vol. **12**, No. 4, pp. 984-995, 1996.

Moeller, C. C., W. P. Menzel, and O. K. Huh: A look at the use of GOES-8 data for monitoring water motions in turbid coastal waters. 8th Conference on Satellite Meteorology and Oceanography, Jan 28 - Feb 2, 1996, Atlanta, GA, AMS, 435-438, 1996.

Moeller, C. C., O. K. Huh, W. P. Menzel, and H. H. Roberts, The use of aircraft-borne MAS data for mapping sediment transport along the Louisiana Coast. *Second International Airborne Remote Sensing Conference and Exhibition*, 24-27 June 1996, San Francisco, CA, ERIM, Vol. II, pp. 673-682, 1996

Moeller, C. C., O. K. Huh, and W. P. Menzel: Coastal zone applications of MODIS from aircraft and satellite. Workshop on Natural Coastal Environmental Hazards, Feb. 22-23, CSI Tech Report TR-654, pp. 119-123, 1996

IV. REFERENCES

Gordon, H. R., D. K. Clark, J. W. Brown, O. B. Brown, R. H. Evans, W. W. Broenkow: Phytoplankton pigment concentrations in the Middle Atlantic Bight: Comparison of ship determinations and CZCS estimates. Applied Optics, 22, 20-36, 1983.

Gumley, L. E., C. C. Moeller, and W. P. Menzel: Monitoring of Mississippi delta coastal geomorphology using high resolution Multispectral Atmospheric Mapping Sensor (MAMS) data. **5th Australasian Remote Sensing Conference**, Perth, Australia, 738-745, 1990.

Guzzi, R., R. Rizzi, and G. Zibordi, 1987: Atmospheric correction of data measured by a flying platform over the sea: Elements of a model and its experimental validation. Applied Optics, 26, 3043-3051, 1987.

Huh, O. K., H. H. Roberts, L. J. Rouse, and D. A. Rickman, 1991: Fine grain sediment transport and deposition in the Atchafalaya and Chenier Plain sedimentary system. **Coastal Sediments '91: Proceedings of Specialty Conference**, June 25-27, 1991, Seattle, WA, American Society of Civil Engineers, New York, NY, 817-830.

Huh, O. K., C. C. Moeller, W. P. Menzel, L. J. Rouse Jr., and H. H. Roberts, "Remote sensing of turbid coastal and estuarine water: a method of multispectral water-type analysis". *J. of Coastal Research*, Vol. **12**, No. 4, pp. 984-995, 1996.

Jedlovec, G. J., K. B. Batson, R. J. Atkinson, C. C. Moeller, W. P. Menzel, and M. W. James, 1989: Improved capabilities of the Multispectral Atmospheric Mapping Sensor (MAMS). NASA Technical Memorandum 100352, Marshall Space Flight Center, Huntsville, AL, 71pp.

King, M. D., W. P. Menzel, P. S. Grant, J. S. Myers, G. T. Arnold, S. E. Platnick, L. E. Gumley, S-C. Tsay, C. C. Moeller, M. Fitzgerald, K. S. Brown, and F. G. Osterwisch, "Airborne scanning spectrometer for remote sensing of cloud,

aerosol, water vapor, and surface properties," *Journal of Atmospheric and Oceanic Technology*, **13**, pp. 777-794, 1996.

Moeller, C. C., L. E. Gumley, W. P. Menzel, and K. I. Strabala, 1989: High resolution depiction of SST and SSC from MAMS data. **Fourth Conference on Satellite Meteorology and Oceanography**, AMS, Boston, MA, 208-212.*

Moeller, C.C., O. K. Huh, H. H. Roberts, L. E. Gumley, and W. P. Menzel, 1993: Response of Louisiana coastal environments to a cold front passage. Jour. of Coastal Research, Vol. 9, No. 2, 434-447.

Moeller, C. C., O. K. Huh, W. P. Menzel, and H. H. Roberts, The use of aircraft-borne MAS data for mapping sediment transport along the Louisiana Coast. *Second International Airborne Remote Sensing Conference and Exhibition*, 24-27 June 1996, San Francisco, CA, ERIM, Vol. II, pp. 673-682, 1996

Roberts, H. H., O. K. Huh, S. A. Hsu, L. J. Rouse, Jr., and D. Rickman, 1987: Impact of cold-front passages on geomorphic evolution and sediment dynamics of the complex Louisiana coast. **Coastal Sediments '87: Proceedings of Specialty Conference**, May 12-14, 1987, New Orleans, LA, American Society of Civil Engineers, New York, NY, 1950-1963.

Stumpf, R. P., "Remote sensing of water quality in coastal waters". In *Proceedings, First Thematic Conference on Remote Sensing for Marine and Coastal Environments*, ERIM, New Orleans, LA, pp. 15-17, June 1992.

Walker, Nan D., "Satellite Assessment of Mississippi River Plume Variability: Causes and Predictability", *Remote Sensing of Environment*, **58**, pp. 21-35, 1996..

APPENDIX A. - NASA SUPPORTED PUBLICATIONS

PROCESS AND CHANGE DETECTION IN COASTAL ENVIRONMENTS: WITH MULTISPECTRAL SCANNERS AND AERIAL PHOTOGRAPHY

O. K. Huh.*, C. C. Moeller#, W. P. Menzel#, and H. H. Roberts*
*Coastal Studies Institute, Louisiana State University, Baton Rouge, La. 70803
#CIMSS, University of Wisconsin, Madison,WI. 53706

ABSTRACT

The Gulf Coast Chenier Plain, a type of coast formed downdrift of major river deltas, undergoes episodes of erosion and deposition variable in space and time. They are controlled by changes in coastal circulation and proximity of delta distributaries. Since 1987, NASA has sponsored several studies of coastal geomorphology and sedimentation as driven by cold front passages. A major discovery has been that the Louisiana Chenier Plain is rapidly evolving from an erosional coast, threatening coastal properties to a depositional one changing into a rapidly prograding, broad, low relief marsh plain and mudflat. The formerly erosional coast is now being "swamped" with fine grained sediment discharged from the nearby, newly invigorated Atchafalaya and Wax Lake outlet distributaries of the Mississippi River delta. Aircraft and satellite borne sensors have enabled us to follow the progress of changes and identify the active processes..

I.0 Introduction

Dynamic air-sea-land interactions in microtidal(15-45 cm) coastal environments result in primacy of atmospheric and river discharge driven processes which: (a) power the oceanic/estuarine circulation, (b) form various coastal water types, (c) distribute suspended and bottom sediments, and (d) drive coastal erosion processes. Sedimentation along the Louisiana Chenier Plain coast is in transition from an erosional to a depositional regime. This transition has been triggered by the following events:

1. extension of the active lobe of the Mississippi to the outer shelf edge, resulting in decreased flow efficiency where a new channel is now favored, that of the Atchafalaya distributary, (see figure 1).
2. the sedimentary infilling of the Atchafalaya River basin, an 180 km long NNW trending topographic low of swamps and lakes filled in with lacustrine deltas(Tye, 1986) and overbank river deposits.
3. The regional coastal circulation with a prevailing westward drift.

The Louisiana-Texas Chenier plain extends from just west of Marsh Island, Louisiana (figure 2) to Galveston Bay. It is a circa 15km wide coastal plain, consisting of an array

* Presented at the Second International Airborne Remote Sensing Conference and Exhibition, San Francisco, California, 24-27 June 1996.

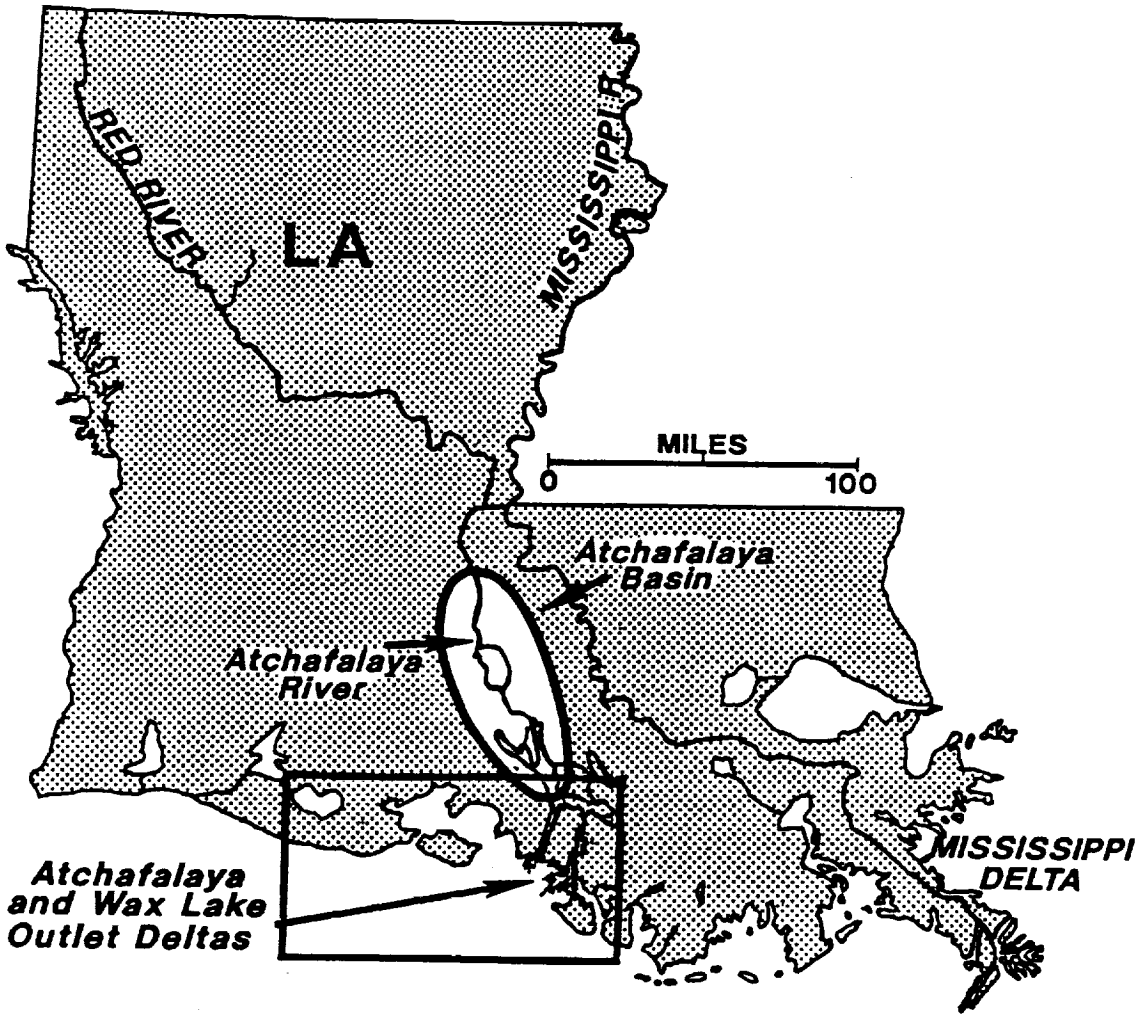

Figure 1. Regional chartlet showing the Mississippi River, the Red River, the Atchafalaya River junction at the old river control structure the Atchafalaya Basin and the Mississippi River Delta.

of nearly shore parallel shell/sand beach ridges(Cheniers) and marsh plant stabilized mudflats. The beach ridges support long linear stands of large, sturdy live oaks that show up in sharp contrast to the marsh grasses. " Chenier" is the french word for "oak", thus the name. The Atchafalaya distributary would easily by now have captured the entire flow of the Mississippi but the negative economic consequences have prompted the Corps of Engineers to erect a control structure allowing 30% of the flow down the Atchafalaya distributary and 70% down the present main channel.

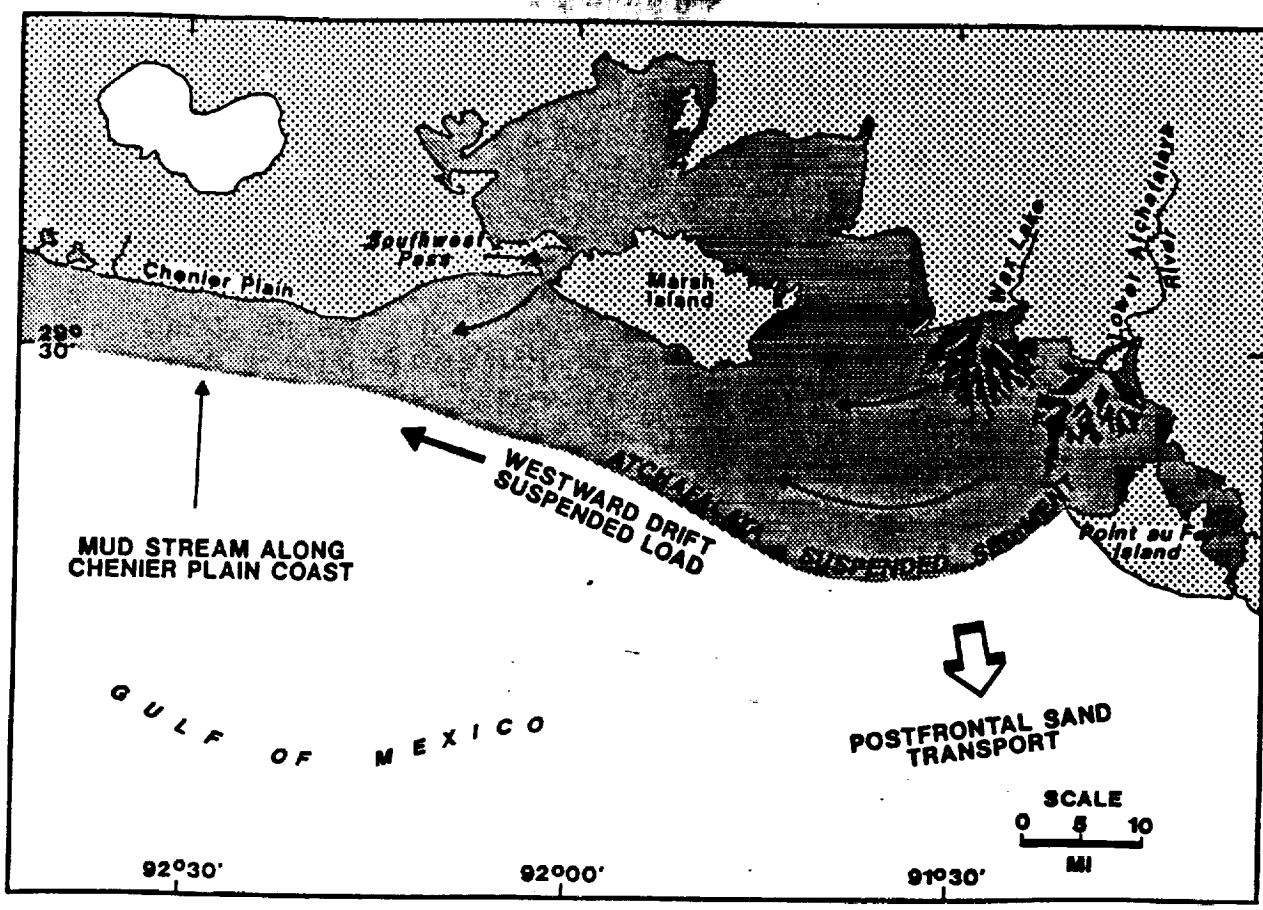

Figure 2. The Atchafalaya mud stream, it origin, path along the coast and the easternmost portion of the Chenier Plain.

The rapid coastal changes have been "tracked" by a series of:

1. ER-2 overflights with Modis Airborne Simulator(MAS), Multispectral Atmospheric Mapping Sensor(MAMS), and color aerial photography.
2. Learjet overflights at two altitudes, 6000ft and 39,000ft with the Calibrated Airborne Multispectral Scanner(CAMS) plus aerial photography
3. Surveillance of coastal and continental shelf waters via NOAA satellite AVHRR imagery using water temperature and turbidity measurements to track the transport by coastal mudstreams.
4. multiple ground truth field trips.

This study is focused on a once every 1000 years geological event; the abandonment of one major delta lobe(the present birdfoot delta) and the birth of a major new delta lobe by the Atchafalaya distributary. . Here, for the first time we observe the earliest phases of a delta lobe shift, which involves a massive transfer of water and sediment from one lobe to another by "stream capture". It is taking place in "slow motion" due to man's interference, but allows

us to follow and document the progress carefully, and to understand these earliest deposits. These are perhaps most likely to be preserved in the geological record, protected from erosion by massive later deposits accumulating above and to seaward.

2.0. THE COASTAL CURRENT AND THE ATCHAFALAYA MUD STREAM.

The new growth of the Gulf Coast Chenier Plain receives its essential sediment supply from the waters and sediments of the Atchafalaya Distributary that are injected into the westward flowing coastal current. The river outflow is normally a stream of muddy water, the "Atchafalaya Mud Stream"(Wells and Kemp, 1981) entrained in the coastal current. It becomes a discharge "plume" only when it flows offshore during slack current periods or when it is driven offshore by Northerly winds.

2.1. THE ROLE OF COLD FRONT PASSAGES

The flow of the coastal current and the cool, turbid waters of the Atchafalaya mud stream are clearly visible in the Advanced Very High Resolution Radiometer imagery (figure 3). Cold front passages are major atmospheric forcing processes that provide for a sequence of events that includes:

1. Pre-frontal strengthening of southerly winds, increased wave action on the coast and continental shelf, setup of sealevel, spillage of inner shelf waters into estuaries, resuspension of sediment and a temporary warming trend.

2. Overrunning by a frontal passage squall line, a zone of extreme atmospheric turbulence, strong and variable winds, much oceanic and estuarine vertical mixing, sediment resuspension, and rainfall.

3. Cold Air outbreak behind the cold front passage. Conditions change rapidly to strong northwesterly winds which are cold and dry, which continue forcing vertical mixing processes, chilling of shallow waters, forcing of sealevel downward to spill the sediment laden waters out of the estuaries into the inner shelf environment. These latter winds temporarily reverse the prevailing coastal current from its westerly flow direction to southeasterly direction. Following most cold fronts a significant SE oriented discharge plume may be seen from the mouth of the Atchafalaya Bay (figure 3a). (Huh, Rouse, and Walker, 1984,and Huh, et al, 1991)

These processes repeated 30-40 times per year combined with the high sediment loads of the Mississippi distributaries(100,000 tons daily ranging up to 300,000 tons daily in flood season), are coastal processes of fundamental importance to this region. They force

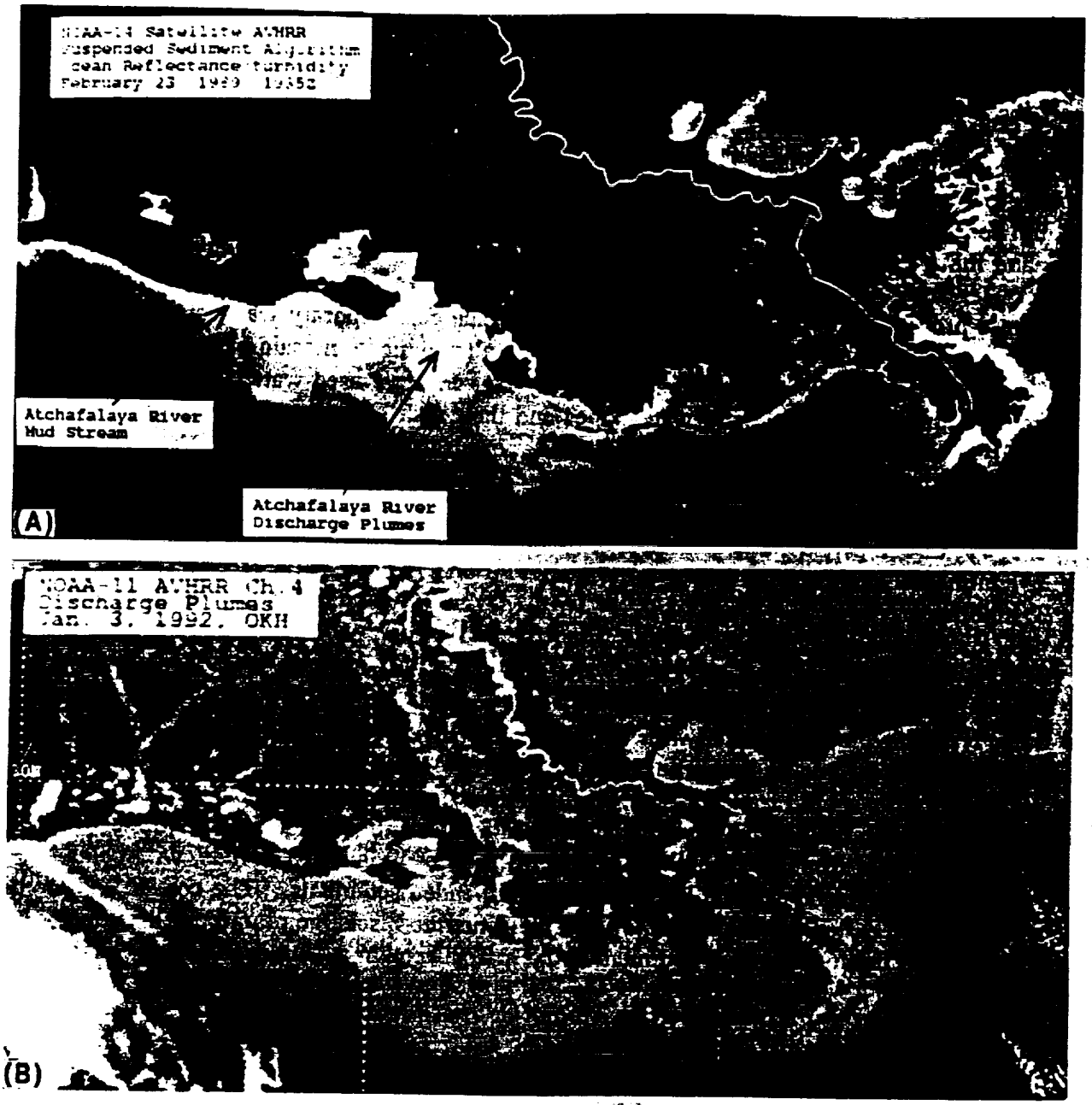

Figure 3a. NOAA Satellite Advanced Very High Resolution Radiometer image of the coastal waters. This image is a calculated water leaving reflectance calculated by subtraction of AVHRR channel 2 from channel 1 and applying an aerosol correction (Stumpf and Pennock, 1989).
3b. NOAA satellite AVHRR thermal image showing the cold coastal current and its westward drift.

exchanges of water and sediment between the inner shelf and the rivers/estuaries of the region. During the sea level setup period they block the river discharge and back these fresh, sediment laden waters into the coastal marshes and wetlands. When sealevel is set down, these waters drain seaward, leaving most of their sediment loads among the roots of the marsh grasses which act as filters. This replenishes nutrients of the wetland soils and contributes to regional sedimentary upbuilding(Reed, 1989). Reed further finds that "Maximum sedimentation is associated with strong southerly winds both causing increased flooding and mobilizing sediment from open bay areas."

These processes of river runoff, storm driven exchange, temporary water storage, storm surges, important water level rise and fall events, all produce a mosaic of coastal water types in this coastal area. Without a reliable salinity tag, we have used water temperature and turbidity to quantitatively classify water types and their distribution patterns to identify sources(Huh, et al, 1996). We have five recognizable types in the vicinity of the Atchafalaya Bay and river mouth:

1. River discharge waters
2. continental shelf waters
3. ambient bay waters
4. Marsh drainage waters
5. soil water

These water types have been detected with the Multispectral Atmospheric Mapping Sensor(MAMS) and the Modis Airborne Simulator(MAS). They are most clearly differentiated just after a cold front passage, readily detectable through the clear dry air of the cold-air-outbreak and largely cloudless atmospheric high pressure system. In the quiescent period following a cold front passage, the physical differences progressively fade, with solar warming of surface temperatures and settling out of suspended sediments. The coastal circulation returns to a flow to the west and only the estuarine discharge plume that has been driven offshore and the increment of sediment in the marsh remain as evidence of the storm.

2.2 THE ROLE OF RIVER DISCHARGES

The Mississippi River is the sixth largest river in the world in discharge with an annual average flow of 14,000m^3/sec, injecting some 580 km^3/yr of fresh water into the Gulf of Mexico(Walker, et al., 1994). Springtime river flooding, March-May produces the sediment discharge maximum of 300,000 tons daily.. This sediment flood is coincidental with the greatest number of cold fronts that stall in the vicinity of the coast, prolonging the prefrontal conditions of southeasterly winds, which setup the westward coastal flow, strong wave action, and sealevel rise along the coast. The discharged sediments from the Atchafalaya river then flow westward toward the Chenier Plain. The fine grained sediment concentrations in the river range from 250-400 mg/l, but are found to increase to more than 800 mg/l in the mud stream just outside the mouth of Atchafalaya Bay(Wells and Kemp,

1981). The concentrations fluctuate with the discharge of the river, which along with the storms, modulate the volume of sediment rich waters. The mud stream, bypasses Marsh Island and is seen to attach to the eastern-most portion of the Chenier Plain, in the vicinity of Fresh Water Bayou. Along this coast, the shore face is a mudflat, with a 2 to 20m wide fluid mud strip(consistency of heavy cream) just seaward along the coast. Offshore of this fluid mud zone there is a two layer water column consisting of muddy seawater on top and the fluid mud beneath(see figure 5b). The two are distinguishable by the character of the waves that propagate through them. The fluid mud based muddy water transforms wind waves to a parade of long crested solitary waves, the denser fluid mud zone attenuates the waves completely.

3.0 GEOMORPHIC DEVELOPMENT OF THE PROGRADING CHENIER PLAIN COAST

Wells and Kemp(1981) noted that "Deposition of fine-grained sediments from the Atchafalaya mud stream can be noted by the transitory mudflats that have formed along the eastern margin of the chenier plain." This condition continued until 1987, when a dramatic changes took place as mud began to accumulate rapidly along this coast. Over the years between 1987 and 1994, the muddy shore face of the eastern chenier plain began prograding rapidly, at rates of approximately 50 m/yr. Low and high altitude aerial photographs show the rapid progradation and the geomorphic changes taking place(see figure 4a and b, 5a and b, and 6). Figure 4a, representing approximately 1 km of shoreline in winter, 1987 shows the wind waves approaching the shell beach face typical of erosional conditions. Figure 4b shows the same site in 1990, when extensive mud deposits now dominate the shoreface.

Though averaging approximately 50 m per year progradation into the open Gulf of Mexico, this buildup does not occur uniformly along the coast. The mud accumulations occur in a pattern of two arcuate mud bars, convex seaward along the coast, see figure 7 which illustrates one of them. The eastern-most zone of mud accumulation is just west of Fresh Water Bayou, figure 4. Figures 4, 5, and 6 show the progression of seaward progradation, with a transition from a shell beach shoreface(1987) to a zone of mud offshore (1988), to a sparsely plant/colonized mudflat(1990), to a half kilometer band of dense, robust, salt tolerant marsh(see figure 5b). This growth has been rapid and persistent. Two processes are critically important to this land building "event", (a) delivery of the fine grained sediments from the coastal waters to the shoreface and marshy mudflats directly landward, and (b) stabilization of the watery fine grained sediments after deposition.

3.1 DEPOSITION OF FINE GRAINED SEDIMENT AND GEOMORPHOLOGY OF DEPOSITS

Sediment is delivered to the shore face by sealevel oscillations occurring on a variety of scales, from hurricane or winter storm surge, to wave runup. We have observed incident solitary waves runup over the nearly horizontal surface of sedimentation at the shore face. They runup to a stop, instantaneously drop their sediment load, then yield a clear, sediment

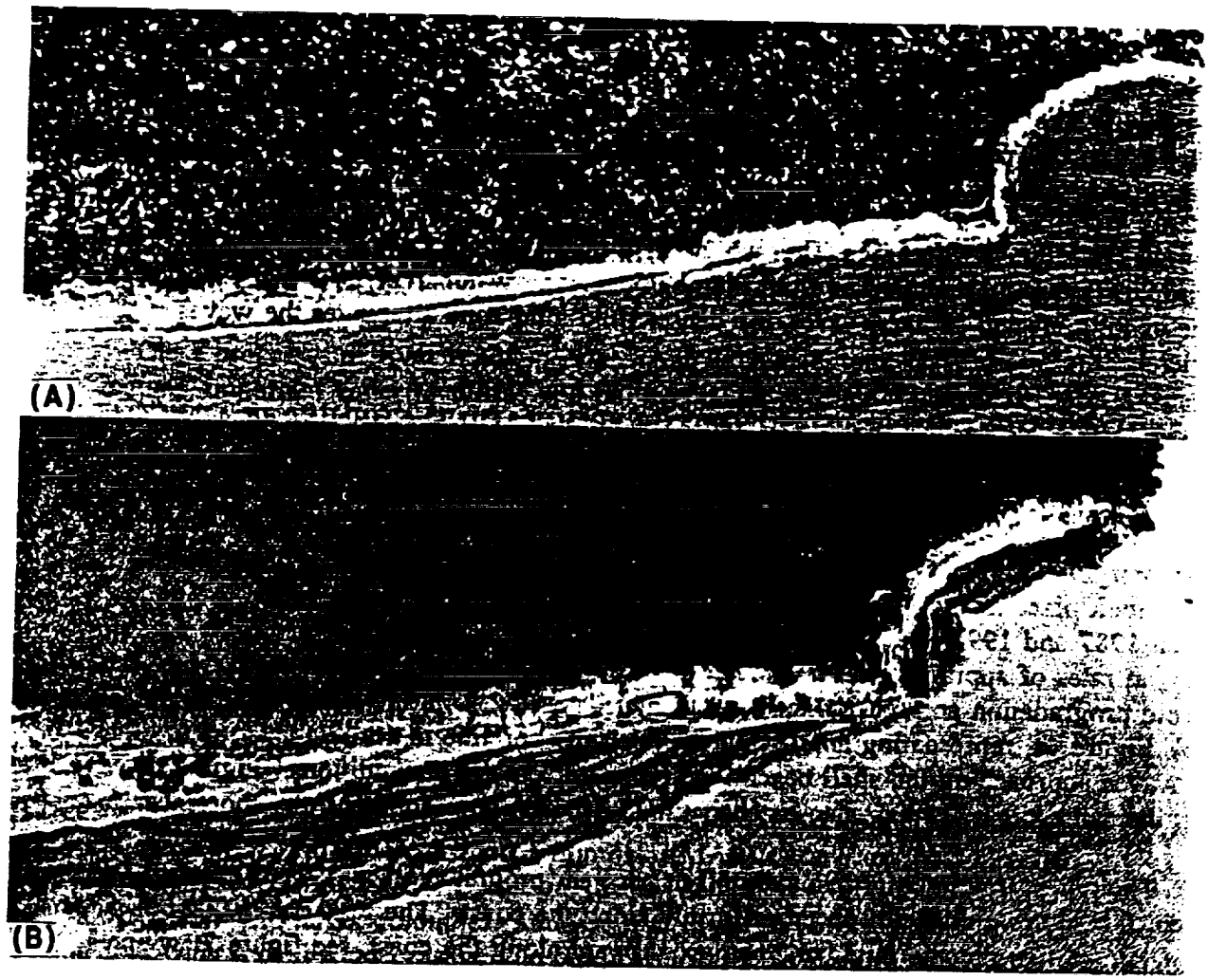

Figure 4. (a) coast just west of Freshwater Bayou, about one kilometer stretch. Note well developed shell(erosional) beach with windwaves approaching the strand. This was flown in Dec., 1987.

4.(b) Same site in 1990, when extensive development of mudflats at the shoreface. marks the transition to an depositional coast due to a flood of fine grained sediment transported hear by the coastal current.

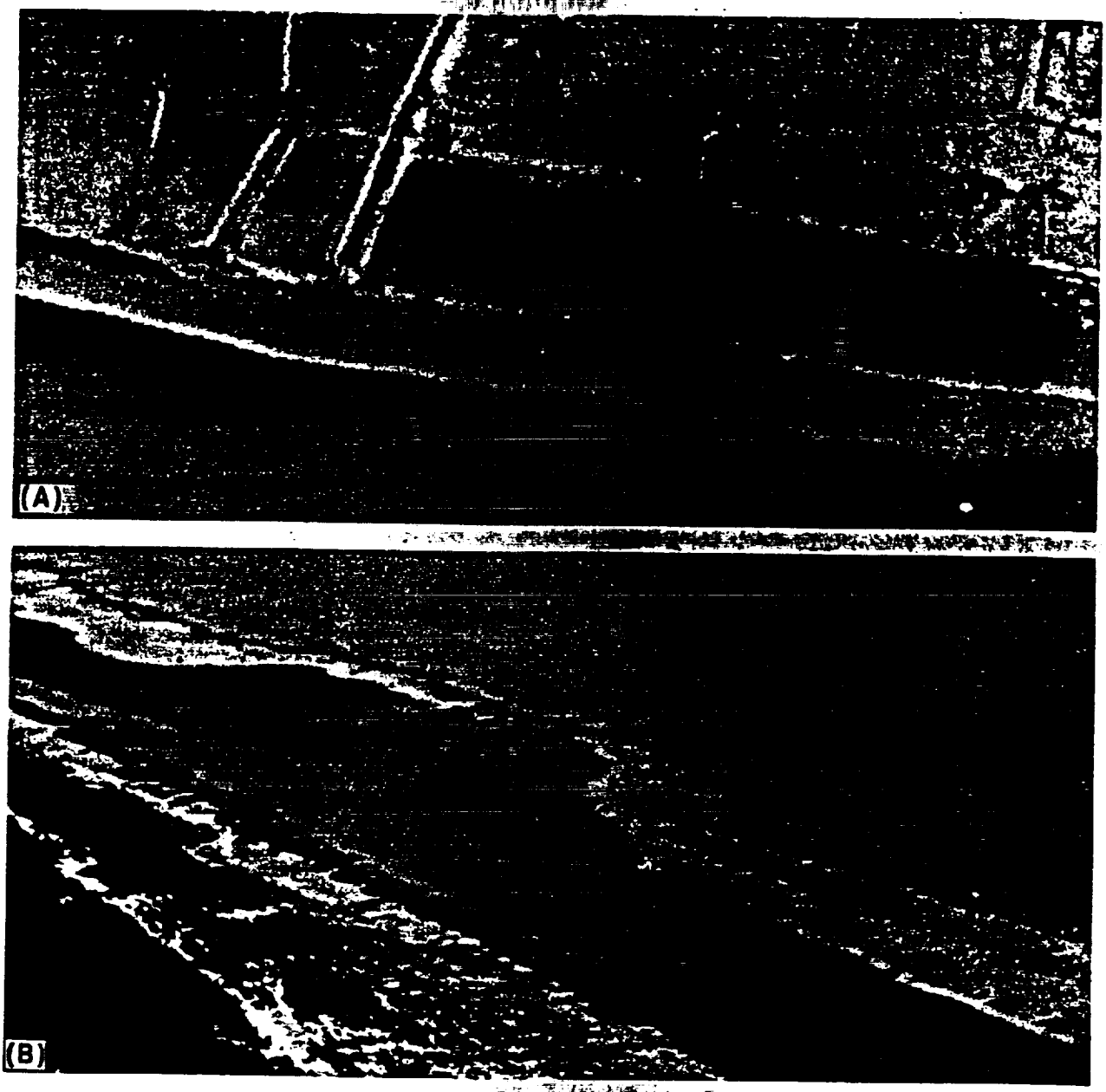

Figure 5. (a) Low altitude(6000ft), 3m resolution CAMS near IR image of the triple canal site 3 km west of Freshwater Bayou. Note the shore-normal canals in the marsh and the linear ponds formed behind the mudbar zone of accretion

(b) Low altitude oblique of the mudbar, shows from lower left to upper right the following features: marsh growth, Shell beach colonized by plants, muddy water of pond behind the mudbar, the mudbar with scattered plants and a thin veneer of fine shell material, a zone of fluid mud at the shore face(with no waves) and then the offshore two layer water column with solitary waves propagating landward.

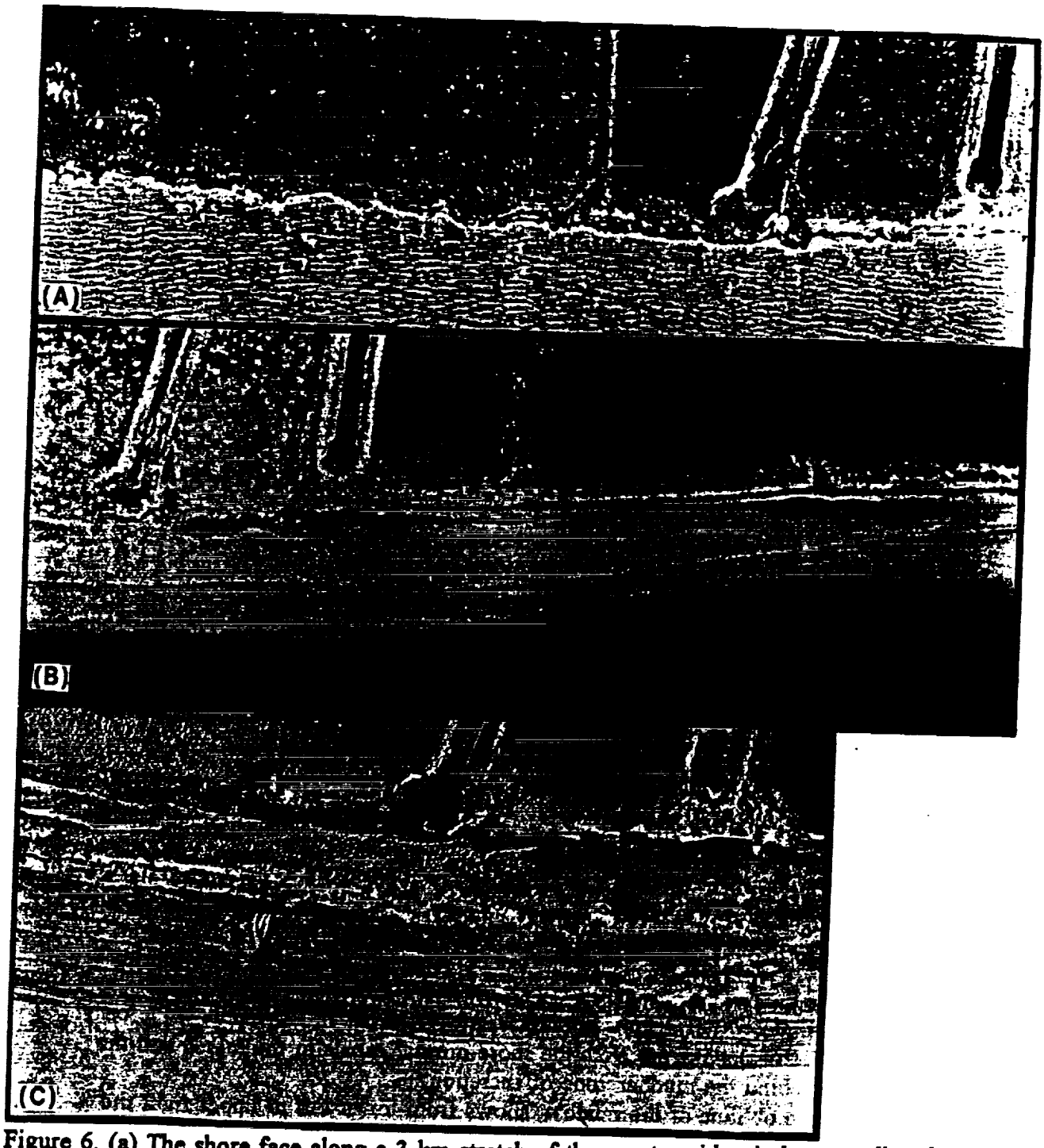

Figure 6. (a) The shore face along a 3 km stretch of the coast, with wind waves directly impacting the strand, Dec, 1987.
(b) The newly deposited fluid mud along the coast, January, 1988, no plant colonization.
(c) The same site in 1990, with extensive development of the mud flats with linear patterns of mud deposition. Plant colonizations on the landward side against the canal endings.

free backwash into the Gulf. We have observed deposition on a cm scale, side by side along the coast within 10m, with similar scale wave erosion processes. The difference is deposition sites are fronted seaward with a local bolus of fluid mud and the eroding area, not so protected, is actively eroded by the incident windwaves. After individual cold front passages, we have found fresh sheets of gelatinous mud, both with and without shell sand basal layer. In fact the mudflats are built of these multiple sheets of sediment, as can be seen when wave erosion of the mudflats occur. Mudbars are formed along the coast leaving linear ponds behind the active shore face(see figure 5a and b). The shore face is convex upward in profile when accretion is dominant process and concave upward, when wave erosion is taking place. Hurricanes create either an extreme version of the cold front deposit or if the predominant winds are off shore, i.e. Hurricane Andrew, they create a widespread sheet of fine grained sediments penetrating into the marshy lowlands, with little other discernable change.

3.2 STABILIZATION OF THE DEPOSITS ON THE CHENIER PLAIN SURFACE

The freshly deposited fluid mud is transported landward by the turbulent storm surge overriding previous deposits and penetrating in among the roots of the marsh grasses. In the backwash, seawater outruns the fluid mud, which is trapped by marsh grasses or stranded on the shore face. It has the consistency of "jello" or "tofu" initially, with gravitative water drainage out seaward through scattered channels(see figure 7, small shore-normal channels), by sheet flow, and by wind driven evaporation. This dewatering is the first phase of the consolidation process. The mud cracking process begins on two scales, by dewatering on scale of 20-30cm polygons, and then soon by sun baking, creating polygons of a size controlled by deposit thickness, generally 8-10 cm on a side. They progressively desiccate and the mud beach has been converted to a cobble beach within a few days. Wave action, if any rolls these cobbles around, rounding them, and when rolled over a shell hash, become what is called the "armored mudballs", sticky cobbles of mud that collect a coating of shell fragments. The stabilization process thus involves dewatering, mud cracking, desiccation and hardening of mud "cobbles", which now armor the coast, requiring strong wave action to mobilize. These changes combined with a zone of fluid mud which strongly attenuates the incoming waves clearly demobilizes these deposits. The final stabilization is accomplished by the colonization by Spartina and Panicum sp. marsh grasses, which grow robust and well developed 2-2.5 m tall, nearly impenetrable on foot with tight interlocking root systems that provide strong protection from high wave action. This growth is slack during winter, but spring and summer marsh grass growth are vigorous and extensive. Note, along with the fluid mud brought by coastal currents is the transport of water hyacinth. These floating plants, coming from the Atchafalaya River, are discharged offshore, die from exposure to salt, are carried to the prograding coast by the currents, and are heaved up against the marsh by the ton, creating a natural plant fertilization process. The water hyacinth acts as a fertilizer, armors the coast, and further verifies that the sediment source is truly the Atchafalaya River and not just onshore drift from the continental shelf.

Figure 7. One complete arcuate mud bar, made up of many layers superimposed appears from the air as a highly organized lens, comprised of multiple exposed sheets of muddy sediment cast over the shore face by storm surges. Length of photo 4 km., 1990.

4.0 SUMMARY AND CONCLUSIONS

A major coastal sedimentary and geomorphic event has been "captured" in a series of remote sensing experiments conducted along the Louisiana Coast. A transition from an erosional to depositional coast is taking place in the eastern portion of the Louisiana chenier Plain, still a small portion of the entire Chenier Plain coast. This depositional zone is propagating westward along the coast at a rate of about a km/yr. Using the AVHRR, suspended sediment algorithm, the mud stream of the Atchafalaya River, entrained in the westward flowing coastal current has been identified as the source of a flood of fine grained sediment in this coastal region. This sediment, deposited on the mudflat shore face by waves and storm surges undergo a series of natural consolidation processes which stabilize the newly formed land. These deposits have a seaward progradation rate measured to be ~50 m/year. The most effective storms in this depositional process are the cold front passages, of which some 30-40occur each fall-winter. This is one model of how weather systems of the atmosphere, plus coastal circulation of the hydrosphere organize the architecture of sedimentary deposits, shaping elements of the lithosphere. Remote sensing with scanning radiometers both air and space borne provide essentials on circulation processes, the mud stream, and fine structure of the discharge plume that provides for interpretation of processes responsible for change. For geomorphology, all possible detail is essential, making high resolution aerial photography or very low altitude (< 2000 m) aircraft scanner mission essential for definitive measurements.

5.0 REFERENCES

O. K. Huh, L. J. Rouse, and N. D. Walker, "Cold Air Outbreaks Over the Northwest Florida Continental Shelf: Heat Flux Processes and Hydrographic Changes", *Jour. of Geophysical Research*, Vol 89, No. C1, pp. 717-726, 1984

O. K. Huh, C. C. Moeller, W. P. Menzel, L. J. Rouse, Jr., and H. H. Roberts, "Remote Sensing of Turbid Coastal and Estuarine Waters: A Method of Multispectral Water-type Analysis", *Journal of Coastal Research*, in press, 1996

O. K. Huh, H. H. Roberts, L. J. Rouse, "Fine Grain Sediment Transport and Deposition in the Atchafalaya and Chenier Plain Sedimentary System", *Coastal Sediments '91*,Proceedings of Specialty Conference/WRDiv./ASCE, Seattle, 1991, pp. 817-830

J. Mossa, and H. H. Roberts, "Synergism of Riverine and Winter Storm-Related Sediment Transport Processes in Louisiana's Coastal Wetlands", *Transactions Gulf Coast Association of Geologicl Societies*, Vol. 40, pp 635-642, 1990

H. H. Roberts, O. K. Huh, S.A. Hsu L. J. Rouse. and D. A. Rickman, "Winter Storm Impacts on the Chenier Plain Coast of Southwestern Louisiana", *Transactions-Gulf Coast Association of Geological Societies*, Vol. XXXIX, pp. 515-522

D. J. Reed, "Patterns of Sediment Deposition in Subsiding Coastal Salt Marshes, Terrebonne Bay, Louisiana: the Role of Winter Storms," *Estuaries*, Vol. 12, No. 4, p. 222-227, December 1989.

R. P. Stumpf and J. R. Pennock, "Calibration of a General Optical Equation for Remote Sensing of Suspended Sediments in a Moderately Turbid Estuary" *Journ. of Geophys. Res*, Vol 94, No. C10, pp. 14,363-14,371, Oct. 1989

R. S. Tye, *Non-Marine Atchafalaya Deltas: Processes and products of Interdistributary Basin Alluviation South-Central Louisiana*, Ph.D. Dissertation, Louisiana State University, Baton Rouge, La. 223pp, 1986

N.D. Walker, G. S. Fargion, L. J. Rouse, and D. C. Biggs, "The Great Flood of Summer 1993: Mississippi River Discharge Studied", *Eos, Transactions, American Geophysical Union*, Vol 75, No. 36, p. 409, 414-415, September, 1994.

J. T. Wells and G. P. Kemp, "Atchafalaya Mud Stream and Recent Mudflat Progradation: Louisiana Chenier Plain", *Transactions-Gulf Coast Association of Geological Societies*", Vol. XXXI, pp. 409-416

J. T. Wells and P. Kemp "Observations of Shallow-Water Waves Over A Fluid Mud Bottom: Implications to Sediment Transport", *Coastal Sediments '87", WW Div./ASCE*, New Orleans, LA, pp. 363-378, 1987.

Journal of Coastal Research	12	4	984–995	Fort Lauderdale, Florida	Fall 1996

Remote Sensing of Turbid Coastal and Estuarine Waters: A Method of Multispectral Water-Type Analysis

Oscar Karl Huh†, Christopher C. Moeller‡, W. Paul Menzel‡, Lawrence J. Rouse, Jr.†, and Harry H. Roberts†

†Coastal Studies Institute
Louisiana State University
Baton Rouge, LA 70803,
U.S.A.

‡Cooperative Institute for
Meteorological Satellite
Studies
University of Wisconsin–
Madison
1225 West Dayton Street
Madison, WI 53706, U.S.A.

ABSTRACT

HUH, O.K.; MOELLER, C.C.; MENZEL, W.P.; ROUSE, L.J., Jr., and ROBERTS, H.H., 1997. Remote Sensing of Turbid Coastal and Estuarine Waters: A Method of Multispectral Water-Type Analysis. *Journal of Coastal Research*, 12(4), 984–995. Fort Lauderdale (Florida), ISSN 0749-0208.

Analysis of digital imagery from the 100 m resolution airborne Multispectral Atmospheric Mapping Sensor (MAMS) indicates that scatter plots of remotely sensed sea surface temperature versus visible and near infrared subsurface reflectance can be used to quantitatively distinguish coastal water types. The Louisiana Gulf coast, a complex region of deltas, estuaries, and marshy wetlands, is the setting for this work. Gulf inner shelf and Mississippi River waters are the primary source water types, but four additional water types are formed locally and are readily detectable with MAMS including: shallow ambient bay water, fresh marsh water drainage, salt marsh drainage, and soil water drainage. *In situ* measurements of suspended sediment concentration and sea surface temperature in the Atchafalaya and adjacent bays have verified the characteristics of these water types. It is found that under the forcing of atmospheric cold front passages, water type differentiation is enhanced, creating a mosaic of water types in these coastal waters. Multispectral remote sensing of these complex, variably turbid coastal waters, provides data useful for studies of water type formation and coastal circulation processes.

ADDITIONAL INDEX WORDS: *Atmospheric cold fronts, suspended sediments, coastal circulation, Multispectral Atmospheric Mapping System, SPOT images, atmospheric correction, Aircraft multispectral scanner, Chenier Plain, Atchafalaya Bay, Atchafalaya River.*

INTRODUCTION

Mapping the presence, distribution, and boundaries of various water types is important to a number of problems common to coastal regions around the world. In these environments of complex, time dependant air-sea-river-land interactions, coastal circulation is the essential variable. It is the primary control on physical properties, affecting the fate of toxic pollutants, the movement of fish larvae, the location of fish schools and other marine life, as well as location of erosion and sedimentation sites. The dynamics of coastal and estuarine fronts bounding the water types tend to concentrate water borne pollutants (KLEMAS, 1980).

From space and airborne optical imagery, impressive comprehensive views of coastal waters have been obtained for many years. Aircraft and manned spacecraft photography, and Landsat imagery for example, have provided intriguing color imagery of coastal waters. The coastal region often appears as a patchwork of plumes, mud streams, and zones of various colors and transparencies, distributed from river mouths and surf zones to as far away as the continental shelf edge. However, for most applications, qualitative depiction of color variations is of very limited use. In situ oceanographic analysis traditionally measures temperature and salinity as parameters of primary importance. Without remote salinity sensing systems at appropriate spatial resolution in the near future, water temperature and turbidity/reflectance measurements provide the useful parameters from airborne and spaceborne sensors.

The purpose of this paper is to demonstrate that moderate spatial resolution (100 m or better) multispectral remote sensing of surface temperature and turbidity can quantitatively discriminate water types in complex coastal regions with high levels of sediment loading. The Multispectral Atmospheric Mapping Sensor (MAMS), a multispectral imager that flies on board NASA's ER-2 research aircraft, provides visible, near infrared and infrared thermal imagery at 100 m resolution. This study is an analysis of MAMS data and how it depicts variability of coastal waters. The System Probetoire pour Observatione de la Terre (SPOT), a spaceborne multispectral imager, also provides useful high resolution (20 m) visible/near infrared imagery. While the SPOT data are useful for many inshore studies, the need for a thermal channel restricts it's utility here.

This study is focused on the Atchafalaya-Chenier Plain sedimentary system (HUH *et al.*, 1991) shown in Figure 1. The Atchafalaya River brings 152 km^3 of turbid fresh water

95028 received 10 March 1995; accepted in revision 10 October 1995.

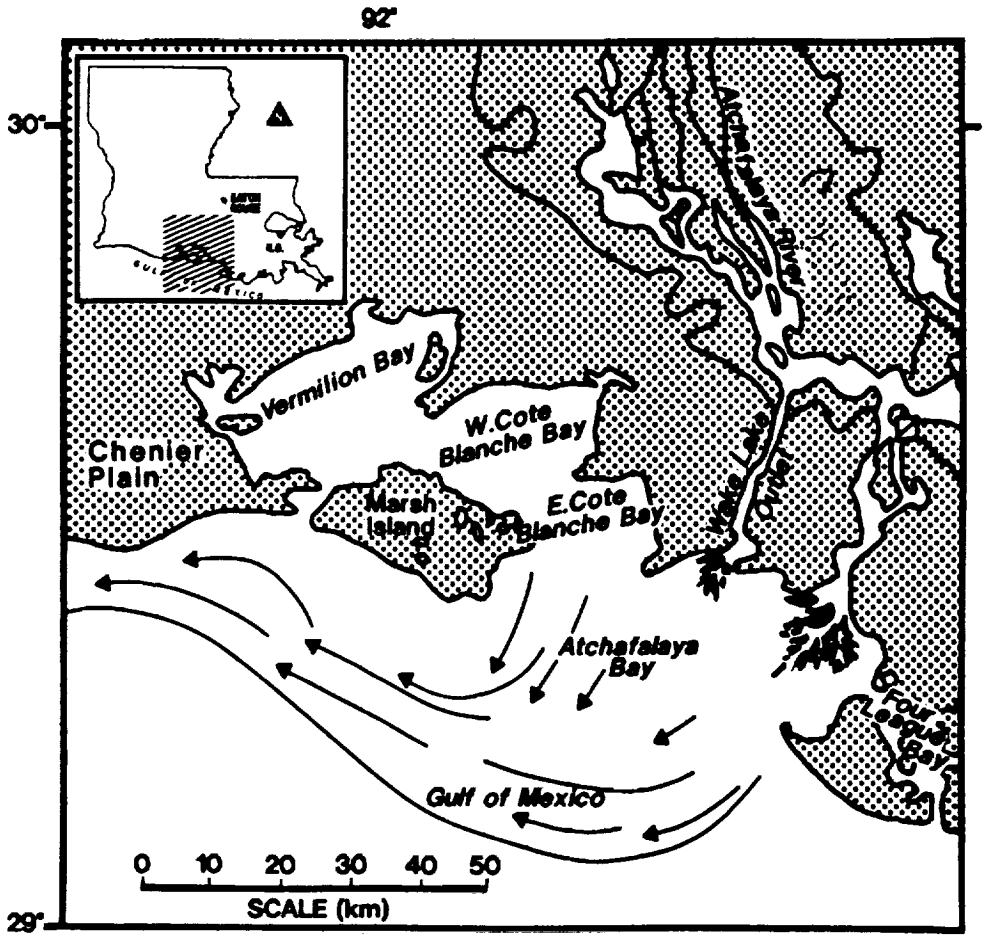

Figure 1. Location map of the study area. The arrows indicate the prevailing transport of surface water and suspended sediment.

(WALKER and ROUSE, 1993) and 88 × 10^6 tons of sediment (ROBERTS and VAN HEERDEN, 1992) into coastal and Gulf of Mexico waters annually (WALKER and ROUSE, 1993). In this deltaic coastal zone, these waters meet in a complex of environments including fresh water marshes, salt water marshes, estuaries, bays, tidal flats, river mouths, deltas and inner continental shelf (Figure 1). Suspended sediment concentrations range up to 1200 mg/l. and more. This coastal region has a broad (100–200 km), shallow continental shelf, is strongly influenced by river runoff, is microtidal (< 1m, semidiurnal), and is experiencing active subsidence (tectonic-compactional-fluid withdrawal) of 1.65 cm/yr. (PENLAND and RAMSEY, 1990). It will be shown that within this complex of environments, atmospherically driven processes alter the physical properties and seston content of local marine and river waters to generate additional water types.

MULTISPECTRAL REMOTE SENSING SYSTEMS, MAMS AND SPOT

A series of 2–4 hour NASA ER-2 aircraft missions have been flown over coastal Louisiana acquiring MAMS imagery and color aerial photography. The MAMS is a cross track, line-scanning, multispectral radiometer (JEDLOVEC *et al.*, 1989; MOELLER *et al.*, 1989). At the operational altitude of 20 km the 5 milliradian aperture yields 100 m resolution at nadir in 12 visible/infrared channels (Table 1). The swath width is 37 km. Calibration of the infrared channels is accomplished by viewing two on-board blackbodies of known temperature during each scan. Visible and near infrared calibration is measured optically in the laboratory before and after MAMS deployments through the use of an integrating sphere at Ames Research Center, California. Voltage output from each MAMS radiation detector is recorded digitally (8 bit precision) on board the aircraft and converted to geophysical units dynamically in the laboratory. A dynamic calibration software package (JEDLOVEC *et al.*, 1989) on the Man-computer-Interactive-Data-Access-System (McIDAS, SUOMI *et al.*, 1983) at the University of Wisconsin converts raw digital counts to radiances for the visible and near infrared channels (channels 2–8) and to radiances and blackbody equivalent temperatures for the thermal channels (channels 9–12). Earth location and rectification of the imagery is accomplished using McIDAS navigation software in conjunction

Table 1. *Specifications of remote sensing systems.*

System	CZCS Bands	MAMS Bands	SPOT Bands HRV	Part of Spectrum
Spectral Bands	1. 0.43–0.45 μm	1. 0.42–0.45 μm		Violet
	2. 0.51–0.53	2. 0.45–0.52		Blue
	3. 0.54–0.56	3. 0.52–0.60	1. 0.50–0.59 μm	Green
		4. 0.57–0.67	2. 0.61–0.68	Yel/Org
	4. 0.66–0.68	5. 0.60–0.73		Org/Red
	5. 0.70–0.80	6. 0.65–0.83		Red
		7. 0.72–0.99	3. 0.79–0.89	Near IR
		8. 0.83–1.05		Near IR
		9. 3.47–3.86		Mid IR
		10. 3.47–3.86		Mid IR
	6. 10.5–12.5	11. 10.55–12.24		Therm IR
		12. 12.32–12.71		Therm IR
Spatial Resolution	825 m	100 m	20 m Multispectral	
Swath Width @ Altitude	1,600 km 955 km	37 km 20 km	60 km 840 km	

with the ER-2 Inertial Navigation System (INS) data. The INS provides aircraft earth position and orientation data recorded at nominal 5 second intervals (JEDLOVEC *et al.*, 1989). For detailed information on the MAMS optical scanning radiometer see JEDLOVEC *et al.* (1989).

SPOT, the French mapping satellite, carries a "pushbroom type imager", an array of charged couple devices (CCDs) which make radiometric measurements in three parts of the spectrum, channels HRV-1 (0.50–0.59 μm), 2 (0.61–0.68 μm), and 3 (0.79–0.89 μm). It provides multispectral digital imagery at 20 m resolution. In waters of low turbidity HRV-3 provides excellent land water discrimination. In these turbid waters it resolves water types containing concentrations of suspended sediment (Figure 2). This system has no thermal infrared sensors for remotely sensing sea surface temperature. The utility of the MAMS data provides a basis for anticipating the utility of the MODIS sensors of the Earth Observing System when they come on line in the late 90's.

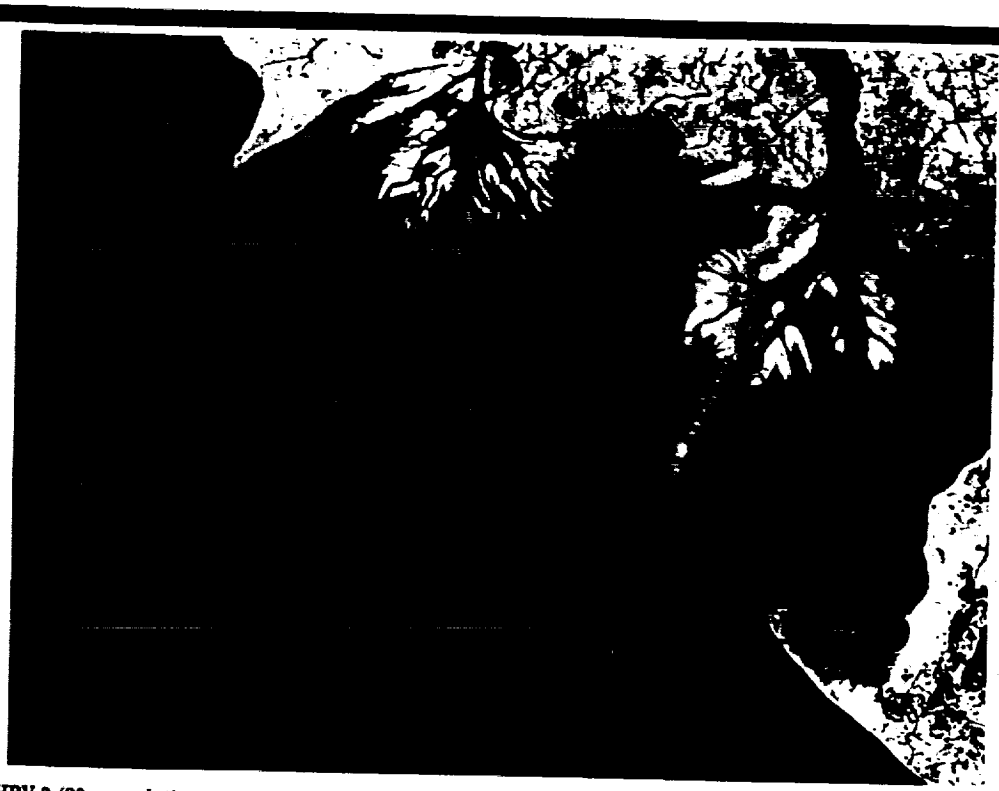

Figure 2. SPOT HRV-3 (20m resolution, near infrared band) image from 27 January 1987: Atchafalaya Bay, the Wax Lake Outlet Delta, and the Atchafalaya Delta. Note the complex patterns of reflectance in the turbid waters of the bay, suggesting an array of water types. The lightest tones are highly reflective areas, land, or highly turbid bay waters.

Figure 3. (a) Image location map; (b) MAMS uncorrected band 3 (.56 μm) imagery; (c) after sunglint removal; (d) after atmospheric scattering removal, leaving an image of scaled water leaving reflectance (x = 500·R). Sunglint correction is not attempted over land surfaces.

ATMOSPHERIC CORRECTION

In order to isolate the upwelling radiance from within the water column, atmospheric contributions to total radiance (molecular and aerosol scattering, ozone absorption) in MAMS visible and near infrared channels are removed using a single scattering model (MOELLER *et al.*, 1993; GUMLEY *et al.*, 1990). The contribution by specular reflectance (sunglint) is estimated using principles outlined in Cracknell (1993), by which it is shown that visible sunglint is related to sunglint at thermal infrared wavelengths. In this case, 11 μm sunglint radiance is assumed small compared to the 3.7 μm sunglint radiance. A difference of the 3.7 μm ($T_{3.7}$) and 11 μm (T_{11}) temperatures is taken as representative of the sunglint at 3.7 μm and the visible sunglint, L_{sg}, for channel k is computed by

$$L_{sg,k} = A \cdot (T_{3.7} - T_{11}) + B$$

The coefficients A and B are determined for each visible/near infrared channel using plots of ($T_{3.7} - T_{11}$) versus visible radiance in regions of sunglint, and fine-tuned by the user through close inspection of the sunglint corrected imagery. Effects by atmospheric water vapor absorption and calibration uncertainty, as well as clear water radiance are implicitly accounted for in the value of B. Instrument viewing angle effects on A and B are not explicitly removed, however, the impact appears minimal as no angular biases are evident in the MAMS atmospherically and sunglint corrected imagery (see example in Figure 3). In this figure, cross track variability is evident on the right side of the images 3b and 3c, in the relatively uniform inner shelf waters. Figure 3d shows a "flat" reflectance field offshore as both sunglint and atmospheric scattering effects have been removed. After correcting for sunglint and atmospheric scattering/absorption effects, the resulting water leaving radiance is converted to a subsurface reflectance ratio (water leaving vs incoming radiance). The procedure is outlined in GUMLEY *et al.* (1990). The

Table 2. *Coastal water type analysis albedo in MAMS Band 6 (0.65–0.83 μm, Red-NIP) vs. water surface temperature.*

Water Types	4 DEC Temperature	4 DEC Albedo‡	5 DEC Temperature	5 DEC Albedo‡	Description
Gulf waters					
Mean	17°C	2%	17°C	2%	Warm, low turbidity
St. D.					
Bay waters					
Mean	8.54°C	12.6%	6.8°C	10%	Cold, very trubid
St.D.	0.15°C	0.1%	0.2°C	0.2%	
River waters					
Mean	11.1°C	9.3%	10.1°C	7.6%	Cool, moderately turbid
St.D.	0.03°C	0.2%	0.3°C	0.3%	
Fresh water marsh drainage†					
Mean	10.2°C	8%	8.5°C	7.2%	Cool, very low turbidity
St.D.	0.4°C	0.3%	0.2°C	0.2%	
Salt marsh drainage†					
Mean	7.9°C	6.5%	6.4°C	7.3%	Cool, very low turbidity
St.D.	0.2°C	0.4%	0.2°C	0.7%	
Soil Waters					
Mean	6.0°C	11.2%	9.3°C	7.8%	Very cold in mid-day, very shallow water environments with variable reflectance, possibly caused by subaqueous bottom reflectors
St.D.	1.0°C	0.8%	1.0°C	0.6%	

‡Calculated subsurface reflectance values (R) converted to albedo by 100*R
†Differentiated by location and source

use of a reflectance quantity as opposed to a radiance quantity is desirable because of varying levels of solar irradiance reaching the sea surface, due to changing atmospheric and local solar zenith angle conditions. Multiplying the subsurface reflectance value by 100 converts it into a more conventional albedo value used in Table 2.

MAMS 11 μm and 12 μm data are used to form a split window correction algorithm to remove atmospheric water vapor absorption effects on MAMS thermal infrared data (MOELLER *et al.*, 1993). The resulting sea surface temperature (SST) is not corrected for emissivity effects due to suspended material in the water; the effect of emissivity variation on MAMS 11 μm and 12 μm data over turbid waters can be reasonably expected to be less than 1 K (WEN-YAO *et al.*, 1987).

METHOD OF MULTISPECTRAL WATER TYPE ANALYSIS

The existence of an inverse correlation between MAMS visible/near infrared reflectances and thermal data in coastal waters was first pointed out by MOELLER *et al.* (1989). Digital interactive inspection of the MAMS subsurface reflectance and surface temperature data revealed considerable variability and much useful detail. Greatest discrimination of water variability details are possible in MAMS channel 6 (near infrared) and in water surface temperatures calculated from the MAMS split window channels. Further evidence of the importance of the near infrared part of the spectrum for highly turbid waters can be seen in the comparison of SPOT HRV-1 (0.50–0.59 μm vis.) and HRV-3 (0.79–0.89 μm near IR) data of Atchafalaya Bay (Figures 4a and b). These two images are greatly enhanced but not atmospherically corrected. The faint vertical striping is due to the fact that extra enhancement has revealed the very small differences (1–2 counts) in sensitivity of the Charged Couple Device (CCD) detectors of the "push broom" HRV sensor. Figures 5 and 6 are paired reflectance-temperature MAMS images from 4 and 5 December, 1990, respectively. The images of both days show zones of uniformity with abrupt boundaries between adjacent bodies of water. The flight of 4 December (Figure 5) occured in post-frontal conditions approximately 12 hours after a cold front passage. Surface winds at New Orleans (MSY) Louisiana, were 7.7–10.2 m sec^{-1} from the north. Water levels in the Atchafalaya Bay were very low due to the combined effects of post-frontal water level set down and low astronomical tide. The 5 December flight (Figure 6) occurred some 24 hrs after a slackening of winds. Subsurface reflectance and water surface temperatures were extracted from the labeled polygons in Figures 5 and 6 and plotted in a temperature/reflectance scatter plot (Figure 7). This diagram is analogous to a temperature/salinity plot used for differentiating ocean waters of various origins. The plot quantifies the separability of the water types. Knowledge of the local sediments and hydrology of the Atchafalaya Bay region along with the reflectance and thermal properties in Figures 5 and 6 allow us to label each water type in Figure 7. The six water types identified are summarized in Table 2. Several of these water types (Gulf, Bay, River) have been identified using suspended

Figure 4. Contrast stretched SPOT images of the Atchafalaya River Delta and a portion of the surrounding Bay: (a) visible "green" band HRV-1 (0.50–0.59 μm), (b) near infrared band HRV-3 (0.79–0.89 μm). Note the greater detail in the HRV-3 image which has *least* water penetration depth. →

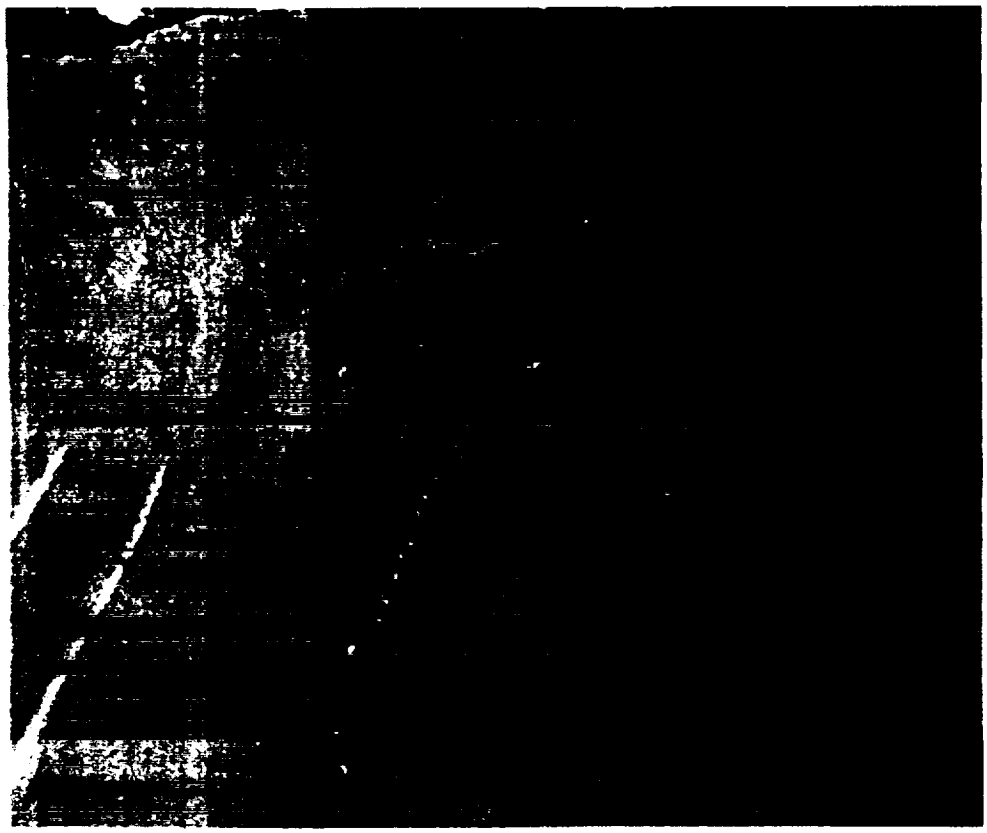

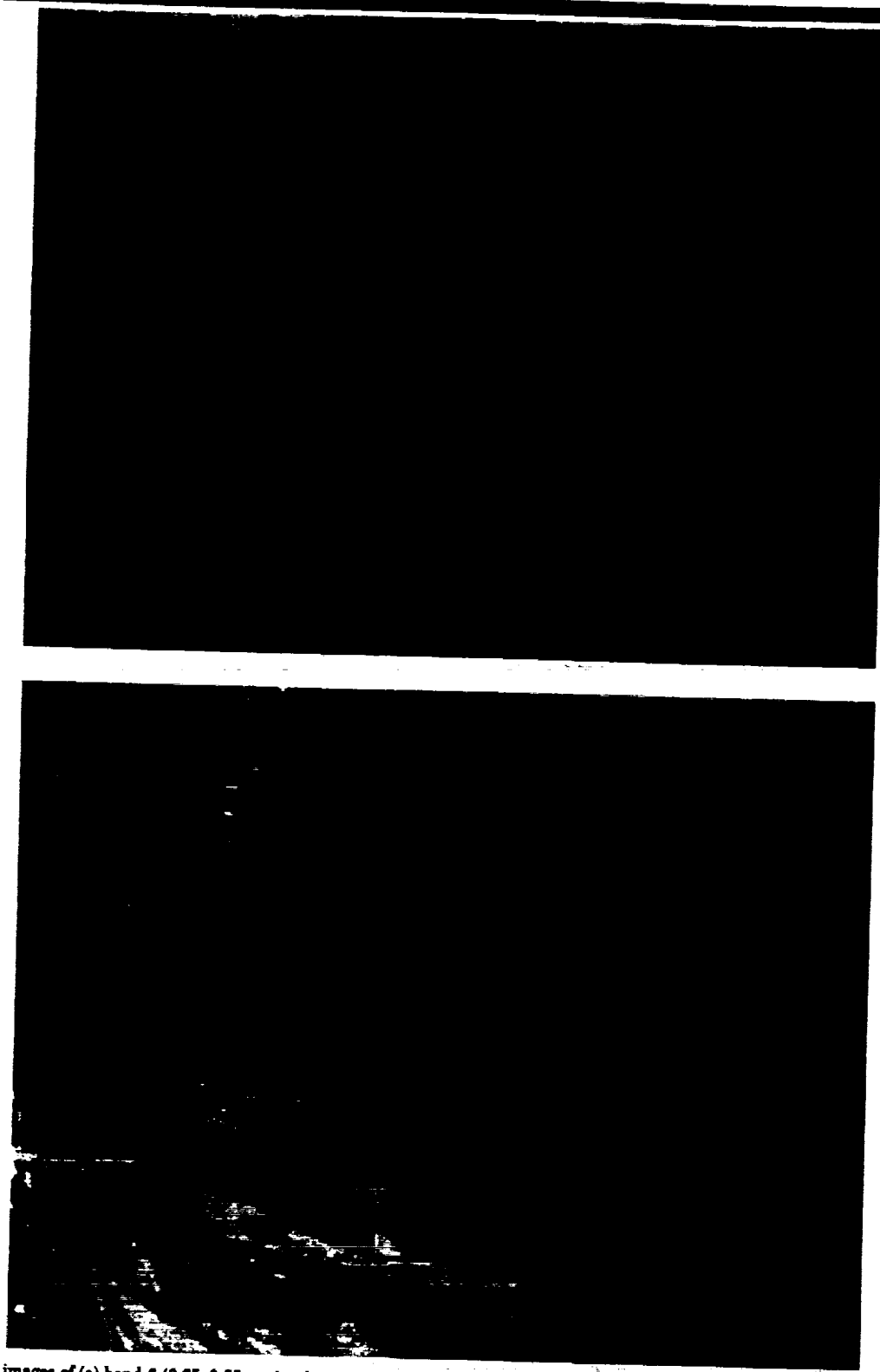

Figure 5. MAMS images of (a) band 6 (0.65–0.83 μm) subsurface reflectance and (b) split window surface temperature for 4 December 1990, approximately 12 hrs after frontal passage. Land reflectance is high (white tones) in the reflectance image. Boxes represent regions of images sampled for 4 December values shown in Figure 7, water types indicated are FM = Fresh Water Marsh; B = Bay water; S = Soil water; SM = Salt Marsh; R = River water.

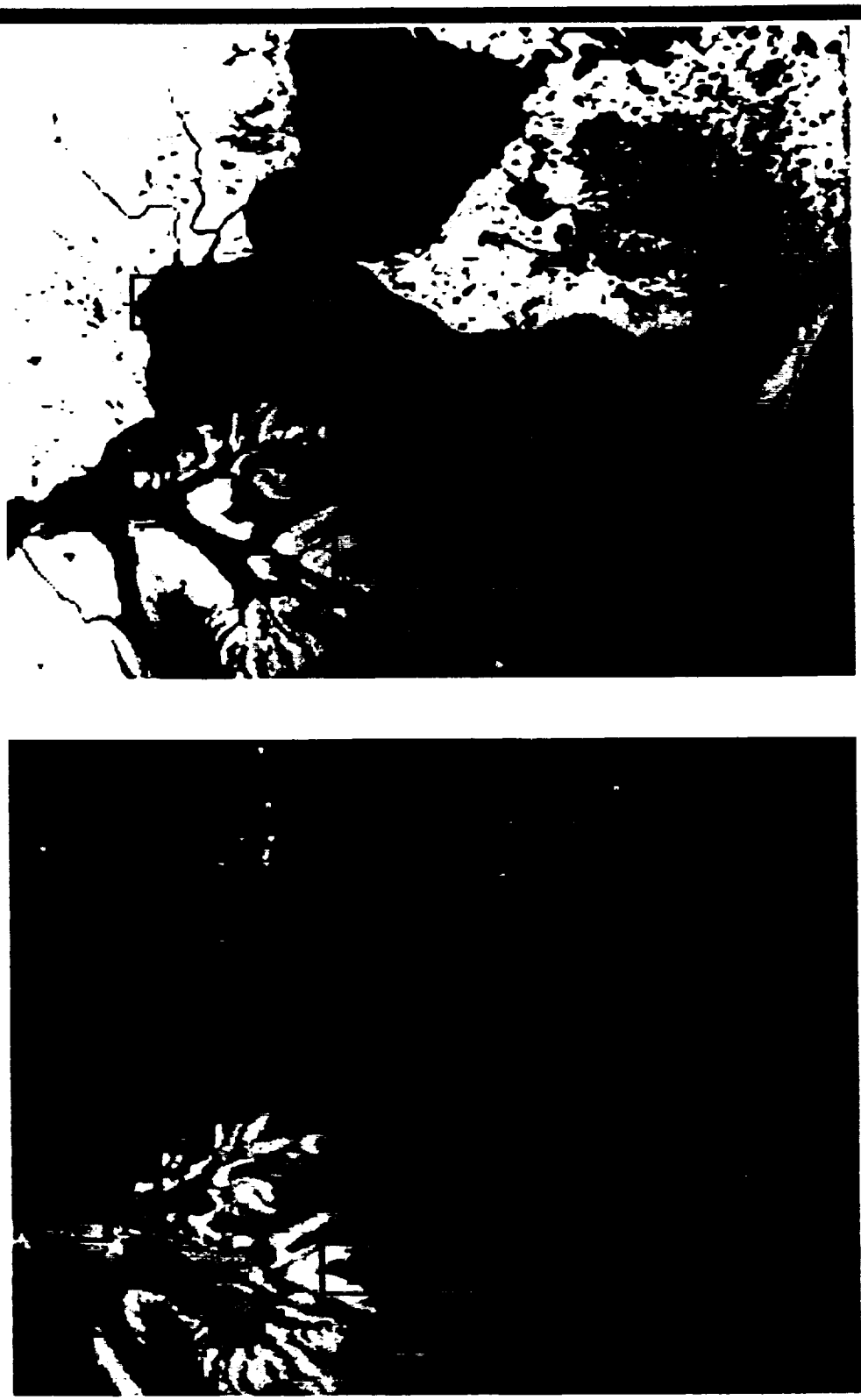

Figure 6. MAMS images of (a.) band 6 (0.65–0.83 μm) subsurface reflectance and (b.) split window surface temperatures for 5 December 1990, some 36 hrs after frontal passage. Boxes represent regions of images sampled for 5 December values shown in Figure 7. Note, although several water types are apparent on both days, there is a general reduction in contrast of water types from 4 December to 5 December, in tandem with a reduction in post-frontal winds and a rise in water level (as evidenced by partial submersion of deltaic deposits in the 5 December imagery.

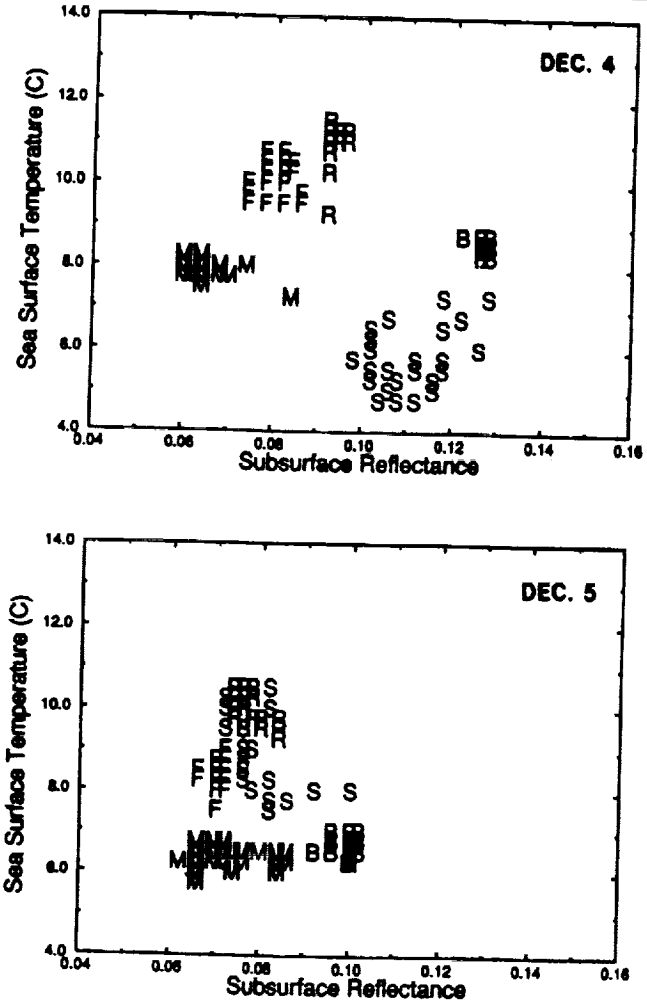

Figure 7. Scatter plots of MAMS remotely measured band 6 (.65–.83 μm) reflectance and split window SST for 4 December (top) and 5 December (bottom) 1990. Data sampled from labeled boxes in Figure 5: F = Fresh Marsh; B = Bay water; S = Soil water; M = Salt Marsh; R = River. Measurements of Gulf waters (not plotted) were 17 °C and 0.02 respectively. Note the clustering of measurements for each water type on 4 December. Some water types also apparent on 5 December, though groupings are more difficult to distinguish. Soil water on 5 December lacks true Soil water characteristics but is plotted as Soil water to demonstrate changing characteristics of colocated waters from 4 December to 5 December.

sediment concentration and SST measurements from a limited in situ data set collected on Dec 4, 1990. It is clear from Figure 7 that a bi-spectral approach aids in the separation of the water types. For example, the reflectance of bay water and soil water are similar; however the temperature signal of soil water clearly separates it from bay water. It should be pointed out that the "spread" of the soil water reflectances may in part be due to bottom reflectance in the very shallow water (< 1 meter) near the delta lobes (clear water penetration depth for channel 6 of approximately 1 m estimated from data provided in MOREL and PRIEUR (1977))

Water types plots for other MAMS visible and near infrared channels were produced and examined. Reflectance variation among water types was much reduced for the shorter wavelength radiation of channels 2 and 3 (blue/green region), and for channel 8, near infrared (channel 7 was not used due to sensor calibration uncertainty). Also channels 4 and 5 (orange/red) showed better differentiation between reflectances of river and fresh marsh waters than channel 6. These spectral dependencies are subjects of future study. The particular characteristics of these water types are dependent on the ambient conditions leading up to and at the time of observation. Seasonal variation in suspended material load and sea surface temperature will shift the plotted points in Figure 6 both left-right and up-down. We suspect that the relative position of each water type will be generally conserved through the cold front season. More observational data are necessary to test this idea.

ATMOSPHERIC FORCING, THE COLD FRONT CYCLE

During the cold front season (October–April), the subtropical U.S. Gulf Coast is repeatedly affected by the trailing edges of passing cold fronts, with mid-latitude cyclones typically tracking further north (PALMEN and NEWTON, 1969). Recent studies (ROBERTS *et al.*, 1987; HUH *et al.*, 1991) suggest that the annual series of cold front passages have as much or more long term impact on these environments than much rarer, but stronger hurricanes. Two important facts about cold-front passage events are: (1) the frequency of occurrence (30–40 yr^{-1}) and (2) the temporally and spatially ordered pattern of change in wind speed, direction, barometric pressure, temperature and humidity. It is important that the orientation of the cold front influences the wind direction, with fronts oriented normal (north-south) to the coast having a very different coastal wind field than those oriented parallel (east-west) to the coast (ROBERTS *et al.*, 1987).

The winter cold front cycle of temperate latitudes is a repeated sequence of events that imparts a burst of kinetic energy and an episode of rapid cooling to coastal and near shore shelf environments. A detailed study of a strong cold front passage and its impact on coastal waters was conducted by HUH *et al.* (1984). From it a simplified descriptive model of a cold front passage event is discussed in ROBERTS *et al.* (1987) and MOELLER *et al.* (1993). A practical consequence of a cold front passage is the regional dominance of a surface anticyclone within a few hours or days. The presence of the anticyclone optimizes optical and infrared remote sensing of the surface by typically bringing cool, dry, cloud-free air over the scene.

Cold front passages appear to play a significant role in the differentiation of water types. The pre-frontal rising sea level drives shelf waters over the shore face into coastal marshes and impedes river discharge into the Gulf. River water and sediment back up into the freshwater marshes and wetlands adjacent to the river channels. During the cold air outbreak phase, sea level set down induces seaward flow of the fresh and salt marsh waters that have been filtered of sediments by flowing through the marsh grasses. These low reflectance waters are routinely seen off Point Au Fer (salt marsh), Four

League Bay, East Cote Blanche Bay, and between the Wax Lake and Atchafalaya Deltas (Figures 1 and 3a). Water held in the sandy deltaic shoals is also released during sea level setdown. The presence of thin streamers of very cold waters from the Atchafalaya and Wax Lake Outlet deltas during mid-day warming was the first clue of this soil water drainage. Bay waters, responding to the cold front passage become colder and more turbid than the river waters, due to strong negative heat fluxes over broad shallow areas and bottom sediment resuspension.

Studies of images and scatter plots indicate that the various coastal waters form, evolve, flow, and generally dissipate in time. The few observations we have now through a cold front cycle indicate that after the initial burst of post-frontal atmospheric forcing, water types are differentiated to a maximum. As the post-frontal forcing weakens (hours to days after cold front passage), waters tend to homogenize. This is due to processes of cold front forced cooling and settling out of suspended sediments. This behavior is apparent in the water types analysis using MAMS data from 5 December 1990 (36 hours after the cold front passage) in Figure 7. Although the 5 December imagery (Figure 6) still shows good variability and indicates the presence of several water types, the plotted sample sites show how the water masses, especially marsh and soil water, have homogenized in both reflectance and temperature to the point that it is difficult to separate the types from one another. This suggests reduced marsh and soil water flow into the bay at the sample sites, a conclusion consistent with increased water levels in the bay. (Observations at New Orleans showed post-frontal winds had decreased to 2.6–5.1 m sec^{-1} from the northeast on 5 December, compared to about 7.7–10.2 m sec^{-1} from the north on 4 December, reducing the water level setdown forcing in the Atchafalaya Bay region.) The combination of reduced marsh and soil flow with the homogenization of water characteristics is probably responsible for the lack of separability in the 5 December plot. Instrumenting key outflow points around the Atchafalaya Bay region would further improve understanding of the impact of cold front passages on the cycle of marsh inundation and drainage, which is a key mechanism by which coastal marshes are supplied with invigorating sediments and nutrients.

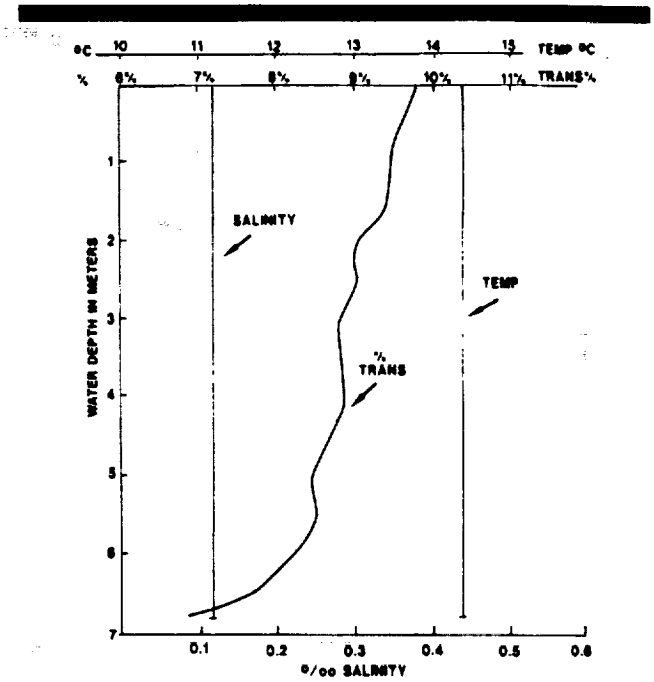

Figure 8. A temperature, salinity, and transparency profile obtained from a research vessel 24 hours after a cold front passage. The plot shows the destratified state of Atchafalaya River Discharge waters in the bay in terms of temperature and salinity with a subtle (3%) change in the transmittance (suspended sediment concentration) profile.

DISCUSSION

For coastal oceanographic applications, important questions are: (a) what is the physical significance of the temperature and reflectance measurements acquired by the MAMS and (b) how well can this instrument remotely measure them? The split window atmospheric correction algorithm allows a calculated estimate of water surface temperature which agrees with in-situ measurements to within 1 °C. However these MAMS radiometric thermal measurements originate from the top 1 mm of the water column. While this leaves the temperature structure of the bulk of the water column unsampled, it has been shown that during cold post-frontal conditions and under tidal stirring, shallow bay (<1 to 6 m depth) water temperatures are vertically well mixed (Figure 8). Thus, particularly under cold post-frontal conditions, one can assume that MAMS SST is representative of shallow bay water column temperature. This is not the case for suspended sediment load.

Reflectance of these coastal waters is controlled by seston content. In contrast to temperature, the reflectance measurements originate from varying levels depending on the scattering/absorption characteristics of the waters as a function of wavelength. For highly turbid bay or river discharge water, the signal originates from the top few decimeters (Figure 9) in most of the MAMS channels. In less turbid waters the signal originates from within the top meter (Figure 9). In shallow bay environments this can result in bottom reflectance being detected by the sensor. For this reason, it is advisable to choose spectral channels in the orange/red to near infrared range for reflectance measurements in bay or nearshore environments. The ambiguity imparted by detecting bottom reflectance possibly contributes to the reduction in reflectance range for the different water types observed in MAMS channels 2 and 3. In addition, vertical reflectance variation in the water column can be expected (see NANU and ROBERTSON, 1990) due to vertical gradients of suspended material. In the case of the Atchafalaya Bay region, vertical variation of water types is plausible as marsh, river, and soil waters drain into and override ambient bay waters. This also contributes to ambiguiety in reflectance observations from spectral channels that "see" further into the water column (*e.g.*, MAMS channels 2 and 3). These arguments suggest the combined use of orange/red - near infrared spectral data with thermal data for identifying water types.

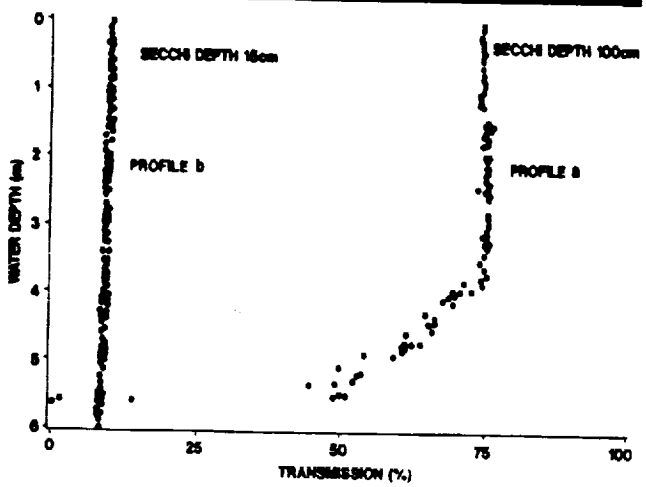

Figure 9. Water transparency profiles and secchi depth measurements in the Atchafalaya Bay before and after a cold front passage. These profiles show the distribution of light scattering particles (suspended sediments) in the water column, in two patterns, (a) pre-frontal pattern, a clear layer (75% transmittance) with a bottom turbid layer (50%–0% transmittance) of entrained sediment from before the frontal passage, and (b) post-frontal pattern, a highly turbid (8%), destratified completely mixed layer after the cold front passage.

Stratified water columns are the norm in the inner shelf seaward of the discharging deltas. The active river discharge plumes are seen to over-run waters of relict plumes (inactive and dissipating) that in turn are overriding warmer, more saline shelf waters. These flow westward with the prevailing coastal current, a flow interrupted by cold front passages that drive episodic eastward flow. The multiple ocean fronts are subjects of further studies.

CONCLUSIONS

Repeated coverage of coastal Louisiana with airborne and spaceborne high resolution multispectral scanner data combined with selective ground truth, is providing a powerful tool for coastal research and an important data base for environmental management. Understanding these complex environments has frustrated conventional data acquisition capabilities for many years. These data are providing an important historical record for analysis of long term changes in geomorphology and hydrology of these rapidly evolving Louisiana coastal-deltaic environments. This record is essential for development of environmental management programs important to sustaining and expanding the regional economy.

From the remotely sensed data and surface observations we recognize the following coastal water modification processes active in these environments:

(1) the rerouting of river discharge waters through fresh water coastal marshes by the damming effect of rising sea levels associated with the pre-frontal water level setup. Filtration of suspended sediment load from river waters by passage through grassy marshes renews marsh growth and reduces the reflectance of fresh marsh waters when they drain in post-frontal conditions,

(2) the flow of suspended sediment rich, inshore, marine waters through salt marsh areas, with subsequent filtering of sediment load reducing reflectance,

(3) the resuspension of bottom sediments in shallow waters of estuaries and river mouths, through cold front driven wave and current action, increasing bay water reflectance,

(4) the entrapment of river or estuarine waters as soil water within the sand banks of the newly formed deltas. These waters drain seaward under very low sea level stands associated with the cold air outbreak (post-frontal) phase of the cold front cycle. Low temperatures are results of the very short term exposure to solar warming, and

(5) the cooling or heating of standing, shallow surface waters by air-sea heat fluxes, heated or cooled dependant on atmospheric temperatures/humidity, wind speed, water depth, and time in the solar diurnal cycle.

These processes, individually or in combination are the primary generators of the multiple water types detected in the MAMS imagery. With the aid of cold front cycle forcings, these processes are put in motion culminating with an array of water types formed or released into the coastal environments in the post-frontal phase.

Study of these coastal waters through analysis of MAMS imagery reveals two important general facts:

(1) The best information content on these highly turbid (100–1200 mg l^{-1}) coastal waters is contained in the atmospherically corrected MAMS thermal infrared (sea surface temperature from band 11, 10.55–12.24 μm and band 12, 12.32–12.71 μm) and the orange/red-near infrared (MAMS channels 4–6, 0.57–0.67, 0.60–0.73, 0.65–0.83 μm respectively). The SPOT HRV-3 (0.79–0.89 μm) data also gives useful discrimination of water types (Figure 4b) at higher spatial resolution. Obtaining time series images of these data is important for studies of estuarine and coastal processes,

(2) the complex patterns of temperature and reflectance define repeatedly detectable coastal water types, whose source, areal extent, and evolution through time can be analyzed using sequences of this imagery. The MAMS data contains three basic kinds of information useful in identifying water types: temperature, reflectance, and aerial distribution patterns (*i.e.*, dimensions, orientation, boundaries, and associations). Utility of these tools are enhanced when applied in time-series to areally extensive, complex coastal processes.

Making meaningful and adequate measurements within the regional environment has been too costly or impossible with conventional methods. The advent of airborne and spaceborne sensor systems, global positioning systems, and rapid deployment boat operations provide for observations and measurements at the necessary time and space scales, and under conditions not previously possible.

ACKNOWLEDGEMENTS

The authors gratefully acknowledge support from Solid Earth Sciences Branch, Headquarters NASA, contract

NAGW-2052 at LSU and contract NAGW-3318 at University of Wisconsin, the former Office of Space Science and Applications, Headquarters NASA, contract NAGW-1745 at the University of Wisconsin–Madison, and U.S.G.S. project "Critical Processes of Wetland Loss", at L.S.U. Special appreciation is due the pilots and ground crews of NASA's ER-2 aircraft on deployment to the Gulf Coast from Ames Research Center (Moffett Field, CA) and to the Field Support Group of the Coastal Studies Institute for support of surface truth operations.

LITERATURE CITED

CRACKNELL, A.P., 1993. A method for the correction of sea surface temperatures derived from satellite thermal infrared data in an area of sunglint. *International Journal of Remote Sensing*, 14(1), 3–8.

GUMLEY, L.E.; MOELLER, C.C., and MENZEL, W.P., 1990. Monitoring of Mississippi delta coastal geomorphology using high resolution Multispectral Atmospheric Mapping Sensor (MAMS) data. *5th Australasian Remote Sensing Conference* (Perth, Australia), 738–745.

HUH, OSCAR K.; ROBERTS, HARRY H.; ROUSE, L.J., and RICKMAN, DOUG A., 1991. Fine Grained Sediment Transport and Deposition in the Atchafalaya and Chenier Plain Sedimentary System, *Coastal Sediments '91, Proceedings of Specialty Conference* (WR Divin in ASCE, Seattle, Washington, June), pp. 817–830.

HUH, OSCAR K.; ROUSE, LAWRENCE J. JR., and WALKER, NAN DELENE, 1984. Cold Air Outbreaks Over the Northwestern Florida Continental Shelf: Heat Flux Processes and Hydrographic Changes. *Journal of Geophysical Research*, 89(C1), 717–726.

JEDLOVEC, G.J.; BATSON, K.B.; ATKINSON, R.J.; MOELLER, C.C.; MENZEL, W.P., and JAMES, M.W., 1989. *Improved Capabilities of the Multispectral Atmospheric Mapping Sensor (MAMS).* NASA Technical Memorandum 100352, Marshall Space Flight Center, Huntsville, Alabama, 71p.

KLEMAS, V., 1980. Remote sensing of coastal fronts and their effects on oil dispersion. *International Journal Remote Sensing*, 1, 11–28.

MOELLER, CHRISTOPHER C.; HUH, OSCAR K.; ROBERTS, HARRY H.; GUMLEY, LIAM E., and MENZEL, W. PAUL, 1993. Response of Louisiana Coastal Environments to a Cold Front Passag. *Journal of Coastal Research*, 9(2), 434–447.

MOELLER, CHRISTOPHER C.; GUMLEY, L.E.; MENZEL, W.P., and STRABALA, K.I., 1989. High resolution depiction of sea surface temperature and suspended sediment concentrations from MAMS data. *Proceedings, Fourth Conference on Satellite Meteorology and Oceanography* (American Meteorological Soc. Boston, pp. 208–212.

MOREL, A. and PRIEUR, L., 1977. Analysis of variations in ocean color. *Limnological Oceanography*, 22, 709–722.

NANU, L. and ROBERTSON, C., 1990. The effect of suspended sediment depth distribution on coastal water spectral reflectance: Theoretical simulation. *International Journal of Remote Sensing*, 14(2), 225–239.

PALMEN, E. and NEWTON, C.W., 1969. *Atmospheric Circulation Systems*. New York: Academic, 603p.

PENLAND, SHEA and RAMSEY, KAREN E., 1990. Relative Sea-Level Rise in Louisiana and the Gulf of Mexico: 1908–1988. *Journal of Coastal Research*, 6(2), 323–342.

REED, D.J., 1989. Patterns of sediment deposition in subsiding coastal salt marshes, Terrebonne Bay, Louisiana: The role of winter storms. *Estuaries*, 12(4), 222–227.

ROBERTS, H.H.; HUH, O.K.; HSU, S.A.; ROUSE, L.J. JR., and RICKMAN, D., 1987. Impact of cold-front passages on geomorphic evolution and sediment dynamics of the complex Louisiana Coast. *Coastal Sediments '87*. (WW Div./ASCE, New Orleans, Louisiana, May 12–14, 1987), pp. 1950–1963.

ROBERTS, H.H. and VAN HEERDEN, I., 1992. *Atchafalaya-Wax Lake Delta Complex, the New Mississippi River Delta Lobe.* Coastal Studies Institute Industrial Associates Report, Baton Rouge, Louisiana, 78p.

STUMPF, R.P., 1983. The processes of sedimentation on the surface of a salt marsh. *Estuarine, Coastal and Shelf Science*, 17, 495–508.

SUOMI, V.E.; FOX, R.; LIMAYE, S.S., and SMITH, W.L., 1983. McIDAS III: A modern interactive data access and analysis system. *Journal of Climate and Applied Meteorology*, 22, 765–778.

WALKER, NAN D. and ROUSE, LAWRENCE J. JR., 1993. *Satellite Assessment of Mississippi River Discharge Plume Variability.* Minerals Management Service Report prepared under Interagency Agreement 14-35-0001-30470, 46p.

WANG, FLORA C.; LU, TIESONG, and SKORA, WALTER B., 1993. Intertidal Marsh Suspended Sediment Transport Processes, Terrebonne Bay, Louisiana, U.S.A. *Journal of Coastal Research*, 9(1), 209–220.

WEN-YAO; FIELD, L.R.; GANTT, R., and KLEMAS, V., 1987. Measurement of the surface emissivity of turbid waters. *Remote Sensing of Environment*, 21, 97–109.

P3.16

A LOOK AT THE USE OF GOES-8 DATA FOR MONITORING WATER MOTIONS IN TURBID COASTAL WATERS

C. C. Moeller, W. P. Menzel*, and O. K. Huh+

Univ. of Wisconsin-Madison; Cooperative Institute for Meteorological Satellite Studies
*NOAA/NESDIS/ASPP
+Louisiana State Univ.; Coastal Studies Institute

1. INTRODUCTION

Water motions associated with coastal circulation affect many economic, biological, ecological, and other concerns. For example, timely knowledge of pollutant transport (e.g. oil spills) can be critical to minimizing impact on endangered marine biology. Along coasts of the world, turbid effluent from major river mouths contrasts with clear saline nearshore waters. GOES-8, providing essentially continuous monitoring of North and South America, can potentially track nearshore turbidity contrast for tracers of water motions.

From April 1994 into January 1995, GOES-8 was positioned at 90°W, providing near nadir viewing of turbid waters flowing from the Mississippi River distributary system into the Gulf of Mexico. Transport of effluent from the Atchafalaya River (Figure 1), a distributary of the Mississippi River, has been under study using the MODIS Airborne Simulator (MAS) (King et al., 1995) on NASA's ER-2 high altitude aircraft; turbid plume response to surface winds has been documented (Moeller et al., 1993). In this paper, the use of GOES-8 1 km visible data is explored as a possible source of water motion information along the Louisiana coast. GOES-8 1 km and MAS 50 meter resolution visible data documenting a cold front passage case from January 1995 are examined.

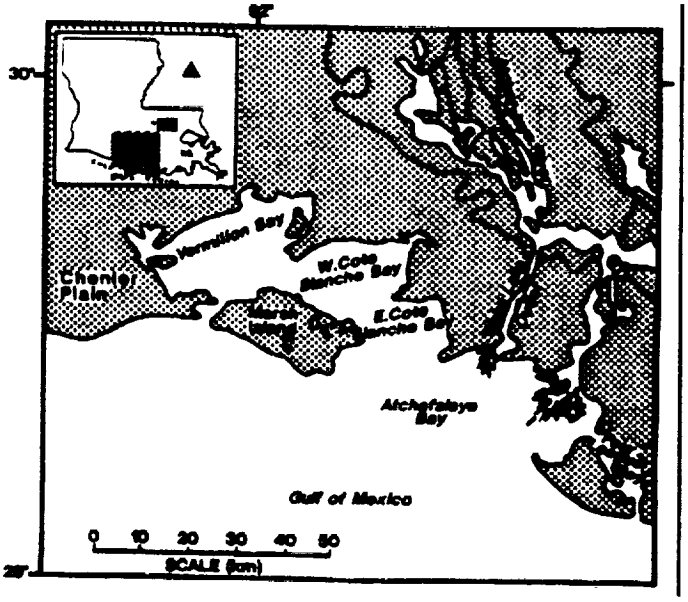

Figure 1. Louisiana coastal region and primary study region for turbid water motions.

Corresponding author address: Christopher C. Moeller; CIMSS, Univ. Wisconsin; 1225 West Dayton Street; Madison, WI 53706-1695

2. WATER MOTION DETECTION APPROACH

Imagery from GOES-8 can be viewed in sequence (looped) using the Man-computer Interactive Display System (McIDAS) at the University of Wisconsin's Space Science and Engineering Center (SSEC). Researchers at SSEC have been active in detecting cloud motions in satellite imagery for more than a decade (e.g. Merrill et al., 1991). Motions are inferred by following trackable features, or targets, from image to image. Targets are tracked either manually (human operator visually tracking targets with a cursor), or by using a variety of automated techniques, most relying on some form of cross correlation statistics. For our exploratory effort into tracking turbid water motions, a manual tracking approach was used. Targets are selected at locations where the water turbidity gradient is large.

The accuracy of manually tracked water motion vectors is limited by image to image registration accuracy, image resolution, and the operator's ability to recognize target displacement from image to image. The GOES-8 imager 15 minute image to image registration performance requirement is 1.5 km and increases to 3 km for a 90 minute interval (Menzel and Purdom, 1994); however, through careful adjustment based on identifiable land features, image to image registration accuracy can be maintained at a sub-pixel level for small regions (such as the Louisiana coast region). For GOES-8 visible data sampling resolution of 1 km north-south and 0.6 km east-west, a sub pixel registration accuracy of 0.5 km and 0.3 km can be achieved. The relative error of the motion vector is the ratio of the registration error over the displacement distance of the vector. Thus, longer time intervals (implying larger displacement) decrease relative error, assuming that a given target is accurately tracked by the operator over the longer time interval. A relative error of 10% requires 5 hour and 3 hour time intervals for a water motion velocity of 28 cm/s (~1 km/hr) in the north-south and east-west directions respectively. Using the 90 minute interval registration performance requirement of 3 km, a 5 hour time interval results in a 60% relative error for a 28 cm/s north-south water motion. Thus, for typical water motions, image registration adjustment reduces the relative error of water motion estimates markedly.

3. RESULTS

Manual tracking was applied to hourly GOES-8 January 23 imagery from 1815 UTC through 2115 UTC. A cold front had passed through the Louisiana coastal region earlier in the morning with clearing behind the front reaching the Atchafalaya Bay region around 1700 UTC. Surface winds of 6 to 8 m/s from the NNW were reported at Lake Charles, LA while instrumentation on an oil platform (29° 32.047'N, 92° 24.814'W) just a few kilometers offshore of the western Lousiana coast reported winds of 10 to 12 m/s from the NNW. In shallow Louisiana coastal waters, post cold front passage winds suppress water levels, pushing water essentially in the downwind direction (shallow water Ekman flow). Figure 2 shows GOES-8 January 23 visible imagery with manually tracked water motion vectors. Relative vector error is ~10-25% for these vectors. While vectors are sparse, a definite indication of water motion in the downwind direction is present. Water appears to be flowing out the mouth of Atchafalaya Bay into the Gulf of Mexico. Figure 3 shows the same display for January 24, a day in which surface winds diminished to about 4 m/s from the NE (oil platform instrumentation) as surface high pressure passed to the north of the gulf coast. Water motion vectors (15:45-17:45 UTC interval) indicate an east to west motion in the nearshore coastal waters, essentially a reversal of the January 23 nearshore flow.

The ER-2 with MAS on board made 3 overpasses of the Atchafalaya Bay on January 24 between 15:30 and 17:30 UTC. Water motion vectors estimated from MAS imagery are shown in Figure 4. Measured MAS registration error (through tracking land motions) indicates ~10-20% relative vector error. It is very evident from Figure 4 that many more targets are identifiable in MAS data. These provide a much larger water motion vector data base and increase the reliability of the estimated water motions through opportunity for nearest neighbor comparison. MAS shows water flowing from the southeast into the western Atchafalaya Bay region, in agreement with the few vectors present in the GOES-8 data set. The general directional pattern shown in the MAS data complements that shown in the GOES-8 data. GOES-8 vector speeds appear to be roughly 25% faster than MAS, a value close to the speed uncertainty of both instruments.

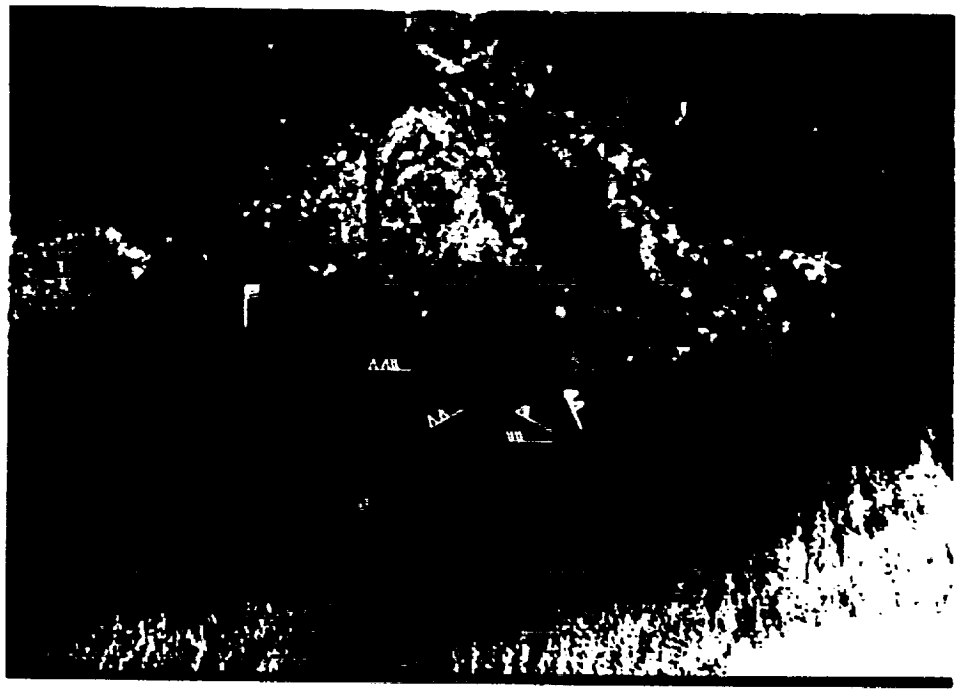

Figure 2. GOES-8 1 km resolution visible image of turbidity pattern along Louisiana coast on January 23, 1995 (20:18 UTC). GOES-8 water motion vectors (cm/s * 2) are shown pointing in direction towards which water is flowing. Water motion towards ESE is apparent on this post-frontal surface wind flow (10-12 m/s from NW) day.

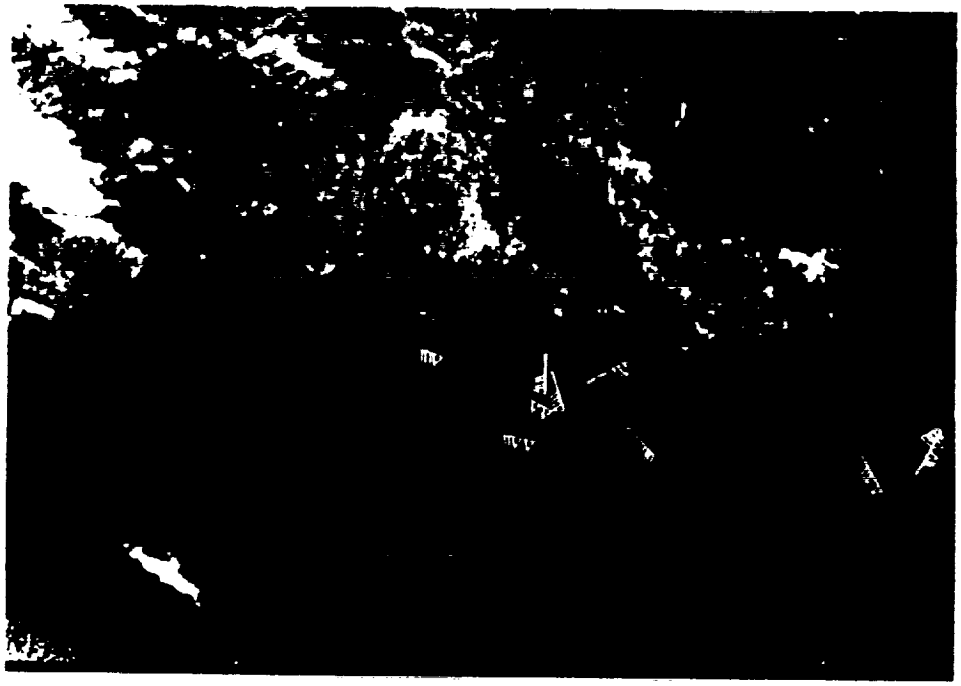

Figure 3. Same as Figure 2 except January 24, 1995 (17:45 UTC). Note reversal of water motions from January 23 1995. Surface winds 2-4 m/s from NE on this day.

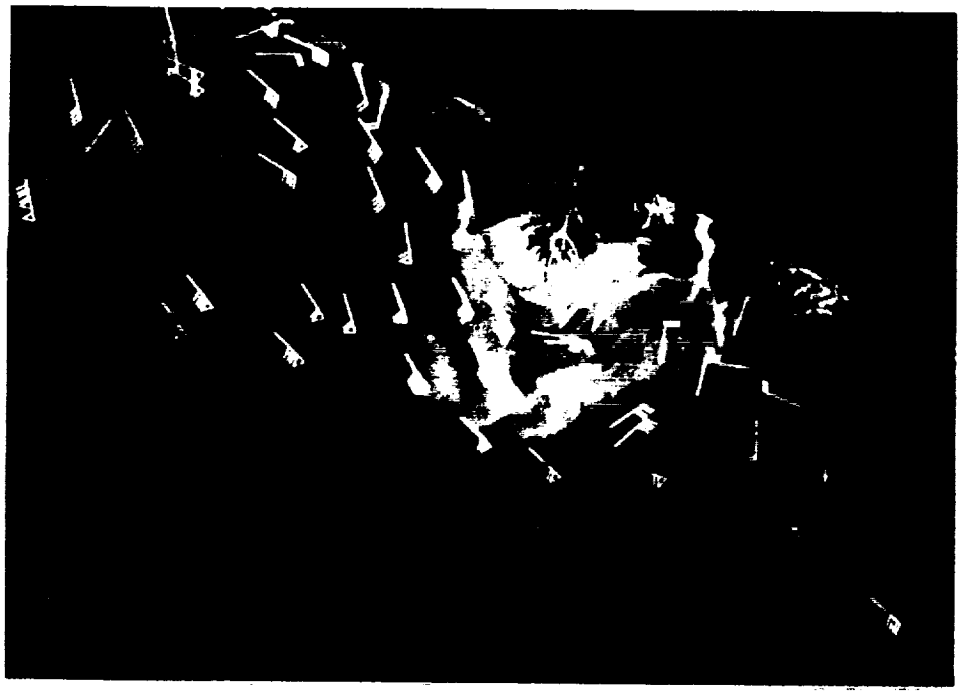

Figure 4. MAS 50 meter resolution visible (0.66μm) imgery on January 24 (17:03 UTC). Water motion vectors (cm/s * 2) show transport patterns in Atchafalaya Bay region (Figure 1) of Louisiana coast.

4. SUMMARY

The contrast of turbid water with clear water in nearshore coastal environments for producing manual water motion vectors is useful with GOES-8 1 km visible data. To achieve good accuracy (10-20%) for typical water motion speeds, it is necessary to improve GOES-8 pixel registration through the use of local landmarks present in the imagery. While unable to resolve the many small scale (< 1 km) targets present in a turbid coastal environment (as shown by 50 meter resolution MAS data), GOES-8 does demonstrate a capability for monitoring general water motion patterns, including an apparent response to a cold front wind system as shown by a reversal of nearshore water motion from January 23 to January 24, 1995. GOES-8 and MAS water motion vectors for January 24 complement each other by displaying transport pattern and general speed estimate agreement (within the limits of vector accuracy). Manual tracking of GOES-8 visible imagery targets will be investigated in the spring season, when distributary outflow is large and nearshore turbidity is high.

5. REFERENCES

King, M. D., W. P. Menzel, P. S. Grant, J. S. Myers, G. T. Arnold, S. Platnick, L. E. Gumley, S. Tsay, C. C. Moeller, M. Fitzgerald, K. S. Brown, and F. Osterwisch, 1995: Airborne scanning spectrometer for remote sensing of cloud, aerosol, water vapor and surface properties. Submitted to *Jour. Atmos. and Oceanic Tech.*

Menzel, W. P., and J. F. W. Purdom, 1994: Introducing GOES-I; the first of a new generation of geostationary operational environmental satellites. *Bull. Amer. Met. Soc.*, 75, 757-781.

Merrill, R. T., W. P. Menzel, W. Baker, J. Lynch, and E. Legg, 1991: A report on the recent demonstration of NOAA's upgraded capability to derive cloud motion satellite winds. *Bull. Amer. Meteor. Soc.*, 72, 372-376.

Moeller, C. C., O. K. Huh, H. H. Roberts, L. E. Gumley, and W. P. Menzel, 1993: Response of Louisiana coastal environments to a cold front passage. *J. Coastal Res.*, 9, 434-447.

THE USE OF AIRCRAFT-BORNE MAS DATA FOR MAPPING SEDIMENT TRANSPORT ALONG THE LOUISIANA COAST*

Christopher C. Moeller[1], Oscar K. Huh[2], W. Paul Menzel[3], Harry H. Roberts[2]

[1]Cooperative Institute for Meteorological Satellite Studies; University of Wisconsin
[3]NOAA/NESDIS/ASPP
1225 West Dayton Street
Madison, WI 53706-1695

[2]Coastal Studies Institute; Louisiana State University
308 Howe-Russell Geoscience Complex
Baton Rouge, LA 70803-7527

ABSTRACT

Sediment-rich effluent from the Mississippi River distributary system flows into clear Gulf of Mexico waters along the Louisiana coast. The sediment, which serves as material for shoreline progradation, is transported by nearshore currents to various portions of the coastal zone. Modis Airborne Simulator (MAS) 50 meter resolution data from NASA's ER-2 platform is used to monitor suspended sediment transport in the Atchafalaya Bay region of the Louisiana coastal zone. MAS repeat coverage visual/near infrared images from a typical 3-6 hour ER-2 mission, are georeferenced, remapped and animated for manual tracking of inwater turbidity features. MAS atmospherically corrected red channel (745 nm) data is used to create estimates of suspended sediment concentration (SSC) using a regression relationship based on in situ SSC samples. The MAS SSC and water motion estimates are combined to produce estimates of sediment transport for the near-surface water column (upper 1 meter). Results for 24 January 1995, a day of light surface winds from the east, show strong transport from the Atchafalaya Bay into the East and West Cote Blanche Bays and relatively weak transport to the Gulf of Mexico continental shelf. Based on previous work, the transport pattern is expected to respond to surface wind forcing, especially associated with the cold front wind system.

1.0 INTRODUCTION

The Louisiana coastal zone is affected by sediment influx from the Mississippi River distributary system. One of those distributaries, the Atchafalaya River, carries high sediment loads (up to 1000 mg/l) into the Atchafalaya Bay region of the coast (figure 1), sustaining a nearshore sediment dominated turbid water mass. Sediment is

---

* Presented at the Second International Airborne Remote Sensing Conference and Exhibition, San Francisco, California, 24-27 June 1996.

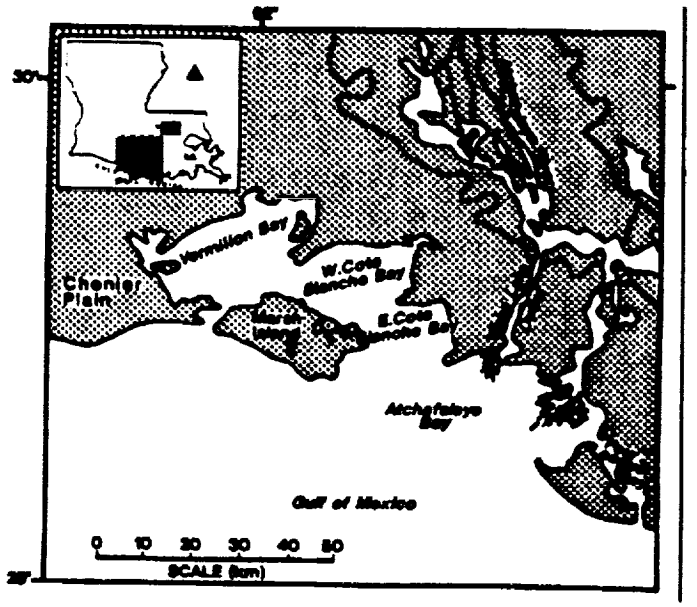

Figure 1. Atchafalaya Bay Region of Louisiana Coastal Zone.

transported variously into coastal bays, estuaries, and out onto the continental shelf of the Gulf of Mexico by variable coastal currents, which are modulated by surface winds and astronomical tides. Previous work has identified new (beginning in 1987) sediment accumulation on coastal shorelines downdrift of the Atchafalaya Bay region (Huh et al., 1991). Moeller et al. (1993) and earlier, Roberts et al. (1987) have indicated that the pattern of sediment transport is strongly affected by surface winds associated with cold front systems. These winds act to drive up and set down water levels in the microtidal Louisiana coastal zone. This paper will focus on the transport patterns on 24 January 1995 as seen by the MODIS Airborne Simulator (MAS) (king et al., 1996). MAS flies on NASA's ER-2 high altitude aircraft, collecting 50 meter resolution data across its 37 km scanning swath in 25 laboratory calibrated visible/near infrared and 25 onboard calibrated infrared channels (Table 1). MAS and , earlier, the MAMS (Multispectral Atmospheric Mapping Sensor) instrument have flown some 20 missions over the Louisiana coast since 1988. Three MAS overpasses of the Atchafalaya Bay over a 2 hour period are used to generate water motion vectors using georeferenced visible/near infrared data; MAS atmospherically corrected visible/near infrared data are investigated to estimate suspended sediment concentration (SSC). These quantities are combined to produce estimates of sediment transport.

2.0 DATA SET COLLECTION

Under clear skies on 8 and 24 January 1995, MAS was flown on the ER-2 over the Louisiana coast. On both days, boat teams from the Coastal Studies Institute (CSI), Louisiana State University (LSU) collected in situ water samples (from top 1 meter of the water column) in the Fourleague Bay region and off the Chenier Plain coast in

TABLE 1. Spectral characteristics of the 50-channel MODIS Airborne Simulator (MAS),

MAS channel	Central wavelength (μm)	Spectral resolution (μm)	MAS channel	Central wavelength (μm)	Spectral resolution (μm)	MAS channel	Central wavelength (μm)	Spectral resolution (μm)
1	0.547	0.044	18	2.030	0.048	35	4.36	0.15
2	0.657	0.053	19	2.080	0.047	36	4.51	0.15
3	0.704	0.042	20	2.129	0.047	37	4.66	0.16
4	0.745	0.041	21	2.178	0.047	38	4.82	0.16
5	0.786	0.041	22	2.227	0.047	39	4.97	0.15
6	0.827	0.042	23	2.276	0.046	40	5.12	0.15
7	0.869	0.042	24	2.327	0.047	41	5.28	0.16
8	0.909	0.033	25	2.375	0.047	42	8.59	0.44
9	0.947	0.046	26	2.96	0.16	43	9.77	0.62
10	1.609	0.052	27	3.11	0.16	44	10.54	0.49
11	1.663	0.052	28	3.27	0.16	45	11.01	0.54
12	1.723	0.050	29	3.42	0.17	46	11.97	0.45
13	1.775	0.049	30	3.58	0.16	47	12.85	0.46
14	1.825	0.046	31	3.74	0.16	48	13.24	0.48
15	1.879	0.045	32	3.90	0.16	49	13.71	0.60
16	1.932	0.045	33	4.05	0.15	50	14.19	0.42
17	1.979	0.048	34	4.21	0.16			

coordination with ER-2 overpasses. Locations of in situ data collection are chosen to maximize turbidity variance, improving the value of the limited sample size (~ 30 samples). On 24 January, the ER-2 flew a racetrack pattern, making 3 overpasses of the Atchafalaya Bay between about 1525 and 1715 UTC (45 minute repeat cycle) (figure 2). Morning data collection was chosen to minimize sunglint in the imagery. Surface winds were relatively light (5 m/s ENE) as atmospheric high pressure lay just to the north. The clear, dry, post-frontal atmospheric conditions optimized the MAS data depiction of coastal water features.

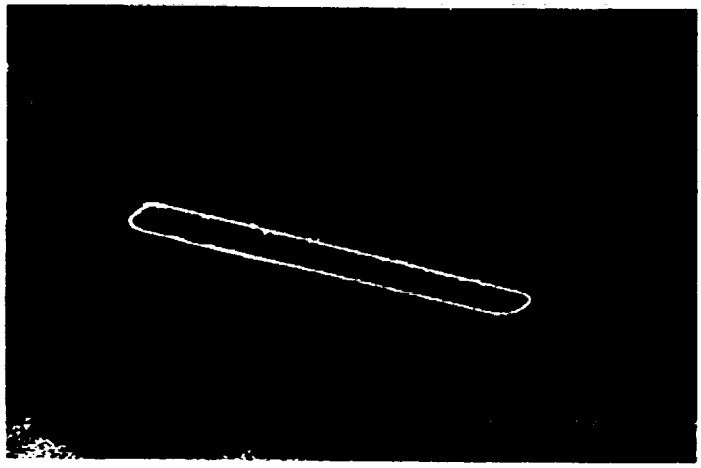

Figure 2. GOES-8 Image on 24 January 1995 with ER-2 Flight Pattern.

3.0 DATA PRODUCTS

3.1 Water Motion Vectors From MAS Data

Tracking water (and atmospheric) features for estimating motion vectors is not new (see recount in Breaker et al., 1994). Historically, both manual (analyst in the production stream) and automated (e.g. maximum cross correlation) techniques have been applied. For estimating water motions with MAS, a simple manual approach was applied to track turbidity features in MAS orange-red (657 nm) and near infrared (869 nm) data. In a manual approach, the analyst subjectively identifies trackable features, determining the feature position in each subsequent image. The MAS imagery are georeferenced and remapped to common projection to facilitate viewing a temporal sequence of images with minimal land motion or "jitter" (during ER-2 flight, data on the three axis (pitch, yaw, roll) aircraft orientation, altitude and nadir latitude/longitude is recorded for use in positioning MAS imagery on the earth geoid). Viewing three or more images in sequence is desirable as the additional image(s) help to fix the feature's progress in the mind of the analyst as well as establish the conservation characteristic of the feature. For the 24 January data set in this paper, a three image sequence was animated on the University of Wisconsin's Man-computer Interactive Data Access System (McIDAS). Velocity vectors are computed from the manually determined position of the feature and associated time data. In the future, automated feature tracking techniques, including feature rotation and deformation (e.g. Kuo and Yan, 1994) will be tested.

3.2 Suspended Sediment Estimate

Isolating the inwater scattered radiance contribution requires the removal of atmospheric scattering (molecular and aerosol) and sunglint contributions to the sensor observed total radiance. MAS visible/near infrared calibrated radiances are atmospherically corrected using the approach outlined in Moeller et al. (1993). This approach is based on single scattering atmospheric modeling work developed by Gordon (1978) and furthered by many (e.g. Gordon et al., 1983, Guzzi et al., 1987). Removing the atmospheric contribution isolates the water leaving radiance (radiance upwelling out of the water column) quantity which is convertible to a SubSurface Reflectance (SSR) quantity following Gumley (1990). The SSR is essentially the water leaving radiance normalized by the solar incoming radiance entering the water column. The 24 January MAS SSR for channels 1-9 (547 - 947 nm) were regressed against the fifteen in situ SSC samples collected in Fourleague Bay. The best relationships were produced by red to near infrared channels (MAS channels 4-6; 745, 786, 827 nm). This is not surprising because the water penetration depth in this region of the spectrum is small (~ 1 meter or less in turbid water), and as such the turbidity signal will originate from a level similar to the in situ samples. Shorter wavelength channels integrate over larger columns and may pick up bottom reflectance in the shallow bay waters, while longer wavelength channels see progressively less of the water column and are adversely affected by atmospheric water vapor absorption in the 900 - 1000 nm spectral region. The channel 4 (745 nm) regression was chosen for application (figure 3). A quadratic provided a good fit of the data, with an RMS of 37.8 mg/l. The 2nd order nature of the SSR-SSC relationship is suggestive of the

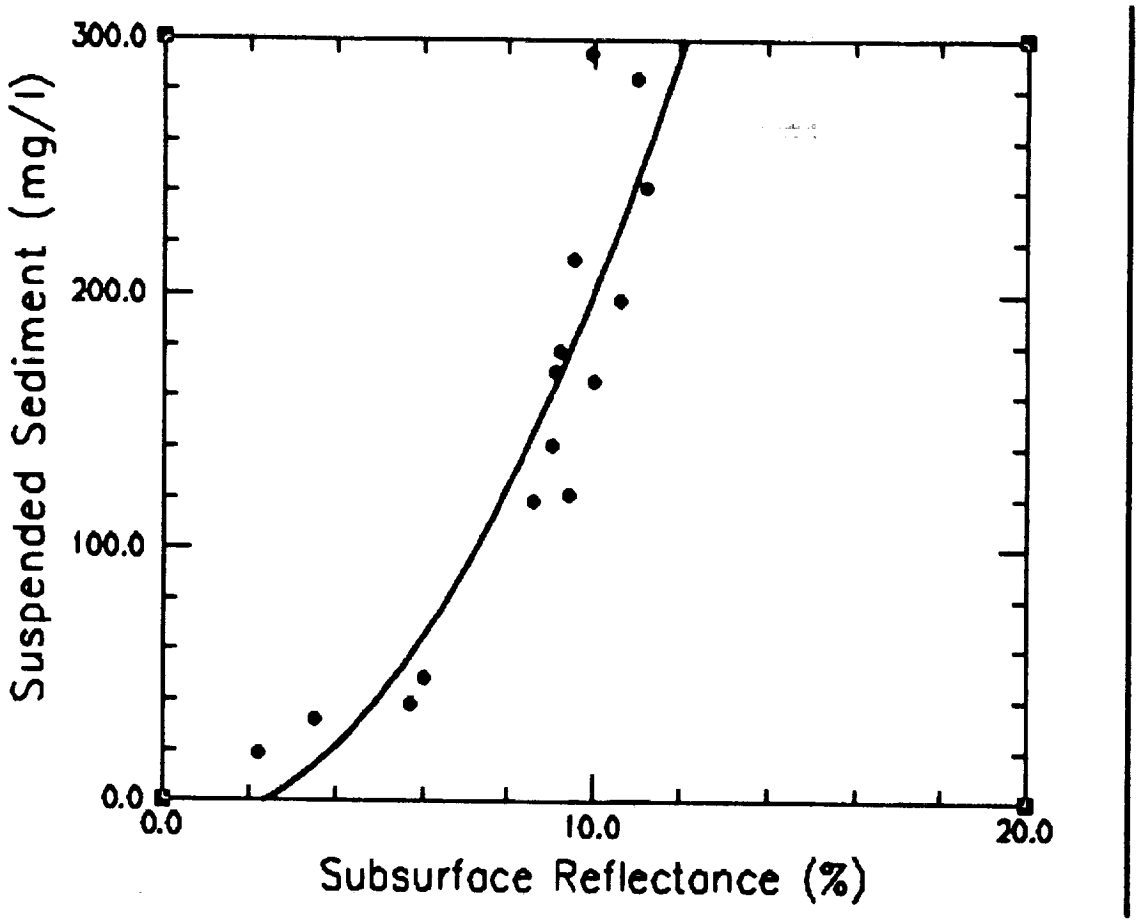

Figure 3. MAS Atmospherically Corrected 745 nm Relationship With In Situ SSC.

nonlinear relationship that exists between optical depth and reflectance in the radiative transfer equation.

3.3 Sediment Transport Estimate

The MAS water motion vectors and SSC estimates are combined with water penetration depth to produce estimates of sediment transport ST,

$$ST(kg/s) = V * SSC * Z * D \quad (1)$$

where V is the water motion velocity (m/s), SSC is the MAS regressed suspended sediment concentration (mg/l), Z is the water penetration depth (m) and D is the MAS footprint width (m). Physically, eqn. (1) represents a sediment transport through the cross section represented by the MAS footprint width and the water column layer from which the sediment scattering signal originates. From work performed by Gordon (1975), Z is estimated to be about 1 meter or less for the MAS red channel at 745 nm. Much of the

Atchafalaya Bay is about a meter or so in depth; surrounding bays (East, West Cote Blanche, etc.) are probably somewhat deeper although good bathymetry for the region is difficult to obtain given the dynamic impact that the sediment influx and resuspension/precipitation processes have on the local bathymetry. As such, the sediment transport estimates reported herein do not necessarily represent full water column transport. However, it is plausible that water motions are fairly uniform in shallow columns (with exception of surface drag at subaqueous bottom), and transmissometer profiles in the Atchafalaya Bay region can be used to model the vertical profile of SSC (they indicate an SSC maximum near the subaqueous bottom which is likely a result of resuspension activity). These assumptions, coupled with good knowledge of the water column depth could be applied to adjust the MAS sediment transport estimates to full column estimates.

4.0 RESULTS AND DISCUSSION

Figures 4 and 5 show water motion velocity and sediment transport data for 24 January 1995, respectively, plotted over MAS remapped SSC imagery. Vector scaling is shown in the figures; vectors point in the direction of flow. For sediment transport estimation, the SSC quantity is averaged over a 3 X 3 pixel box centered at the water motion vector location (base of vector). Water motion velocity relative error (georeference error over the displacement distance) was estimated in the 10-20% range based on tracking land motion in the MAS images. This error translates directly into a 10-20% relative error in the sediment transport estimates as well. It is clear when comparing figures 4 and 5 that relatively high water motion velocity does not imply high sediment transport. It's noteworthy though that the SSC maximum (southwest side of the Atchafalaya Bay) exists in a region of high water motion velocity. The high velocities may be enhancing resuspension activity near this SSC maximum. Outdated bathymetry charts indicate that water depths are about 1-2 meters around the SSC maximum and increase towards the southwest (where velocities remain high but SSC is much lower). A review of MAS imagery collected on 8 January 1995 did not show an SSC maximum at this location; thus it is not likely that this maximum is caused by bottom reflectance. Continuous sediment influx into the Atchafalaya Bay takes place primarily at two locations, the Atchafalaya River and Wax Lake Outlet (located at the right and left newly forming deltas, respectively). A 26.7 kg/s sediment transport is estimated at the mouth of the Atchafalaya River (no trackable feature was available for estimate at mouth of Wax Lake Outlet). Using eqn. (1) and assuming constant water motion velocity and SSC with depth, total sediment transport from the mouth of the Atchafalaya River (~1200 meters wide, dredged to about 15 meters deep for shipping purposes) is estimated at 9612 kg/s. This rate comes to about 3.0e11 kg/yr. Approximating the volume of the high turbidity zone in the Atchafalaya Bay at 20 km X 20 km X 1 meter depth, and using an average MAS SSC of 200 mg/l over this domain, the total sediment load of the Atchafalaya Bay is estimated at 80,000,000 kg. Thus, for the estimated total transport rate at the mouth of the Atchafalaya River, the time required for the Atchafalaya River to replace the sediment load is on the order of a few hours. This simple approximation shows that the sediment transport rate in the Atchafalaya River has a continuous significant impact on the sediment load in the Atchafalaya Bay. Reducing or increasing the sediment transport in the Atchafalaya River

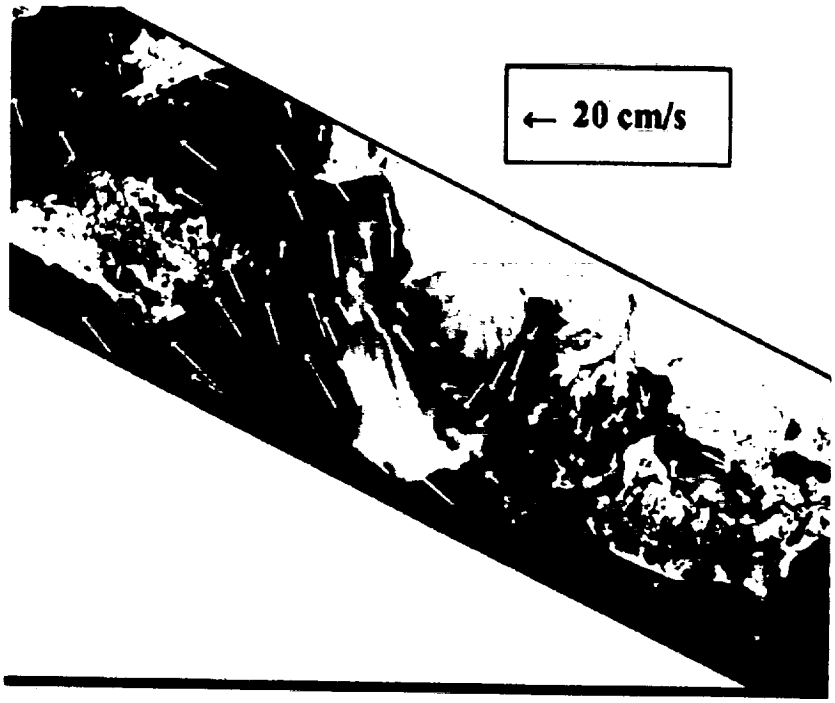

Figure 4. Water Motion Velocity Estimates from MAS 24 January 1995 Data.

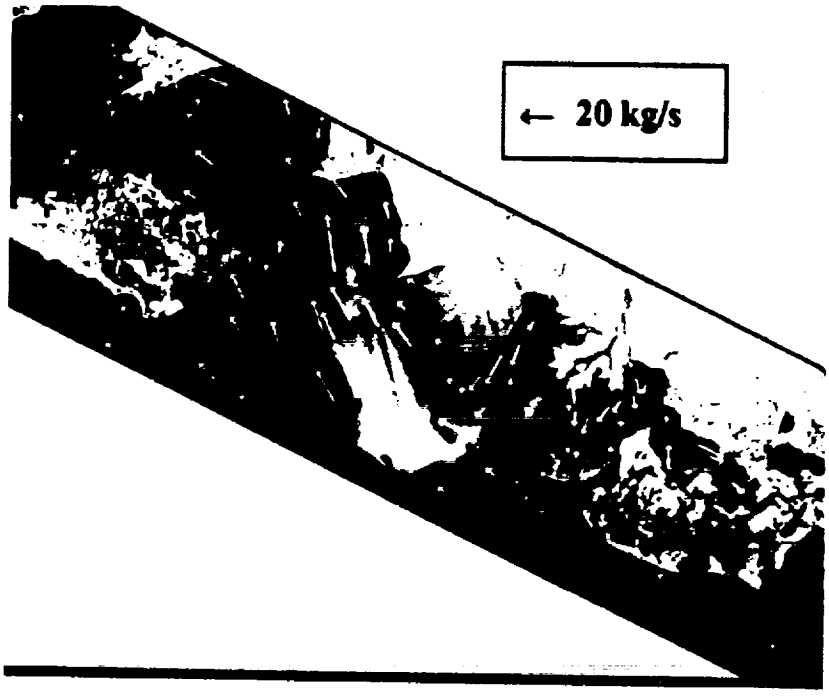

Figure 5. Sediment Transport in the Atchafalaya Bay Region on 24 January 1995.

(e.g. local heavy rains, upstream heavy rain or seasonal drought/flooding) will cause near term variation in the Atchafalaya Bay sediment load (tempered by resuspension/precipitation activity). This sediment load is available for transport to other bays and shoreface. For example, in figure 5, East Cote Blanche Bay is the recipient of strong sediment transport from the Atchafalaya Bay as water velocities in excess of 30 cm/s advect highly turbid water. Water motion velocities and sediment transport in East Cote Blanche Bay are smaller, suggesting a net positive flux of sediment in that region. The Fourleague Bay basin also appears to be experiencing a net positive flux of sediment from the Atchafalaya Bay. No sediment transport from Fourleague Bay into the Gulf of Mexico is indicated through the thin southern outlet connecting them. Instead sediment appears to be transported into waterways on the east side of Fourleague Bay.

Previous MAS (and MAMS) data have indicated that local transport patterns vary greatly in the Atchafalaya Bay region. This has been inferred from variant positioning of SSC maxima and minima as well as through animation of the imagery. SSC maxima have been variously positioned Gulfward over the continental shelf, westward in East and West Cote Blanche Bay and Vermillon Bay, as well as eastward in Fourleague Bay. Obvious indications of SSC transport from Fourleague Bay into the Gulf of Mexico have also been observed. SSC patterns are related to variation of sediment transport from the Atchafalaya River, resuspension activity, and nearshore transport currents (a function of astronomical tides, and atmospheric forcing). A case study in Moeller et al. (1993) showed that southwesterly surface winds retarded sediment transport from the Atchafalaya Bay westward to the Chenier Plain region. AVHRR data have shown sediment transported southward from the Atchafalaya Bay region onto the Gulf of Mexico continental shelf following cold front passages (Walker et al., 1992). Most recently, Moeller et al. (1996) used GOES-8 1 km visible data to show variation in general transport patterns associated with changing surface wind conditions. These investigations point to surface wind as an important influence on transport patterns in and around the Atchafalaya Bay region. In the future, additional MAS data sets will be collected and analyzed for transport patterns and their relationship to atmospheric forcing. In situ data will be expanded to include continuous monitoring of inwater transmission (for SSC data collection enhancement) and the deployment of drifting buoys for estimating water motion velocities.

5.0 SUMMARY

A demonstration using ER-2 mounted MAS 50 meter resolution data for estimating water motion velocity and sediment transport in turbid coastal waters has been presented. MAS georeferenced visible/near infrared data viewed in sequence is used to manually track turbidity features to yield small scale water motion velocity estimates. The ER-2 platform shows itself to be of sufficient stability during repeat flight track coverage to allow the production of useful water motion velocities from MAS data (within 10-20% relative accuracy). MAS atmospherically corrected visible/near infrared data have been used to estimate suspended sediment concentration (SSC) using a regression relationship generated with in situ SSC data collected during ER-2 overflight. The MAS red channel (745 nm) was chosen as producing the best relationship. Sediment transport estimates generated from the water motion velocities and SSC data indicate variable sediment

accumulation in the Atchafalaya Bay coastal region. Such data are informational for hydrodynamic, coastal geomorphic, and marine ecological investigations. The relationship of sediment transport to surface wind forcing, especially associated with cold front wind systems is being solidified by this work and will continue to be pursued.

REFERENCES

Breaker, L. C., V. M. Krasnopolsky, D. B. Rao, and X.-H. Yan, "The feasibility of estimating ocean surface currents on an operational basis using satellite feature tracking methods.". *Bull. of the American Meteor. Society*, Vol. 75, No. 11, pp. 2085-2095, Nov. 1994.

Gordon, H. R., and W. R. McCluney, "Estimation of the depth of sunlight penetration in the sea for remote sensing". *Applied Optics*, Vol. 14, No. 2, pp. 413-416, 1975.

Gordon, H. R., "Removal of atmospheric effects from satellite imagery of the oceans". *Applied Optics*, Vol. 17, pp. 1631-1636, 1978.

Gordon, H. R., D. K. Clark, J. W. Brown, O. B. Brown, R. H. Evans, W. W. Broenkow, "Phytoplankton pigment concentrations in the Middle Atlantic Bight: Comparison of ship determinations and CZCS estimates". *Applied Optics*, Vol. 22, pp. 20-36, 1983.

Gumley, L. E., C. C. Moeller, and W. P. Menzel, "Monitoring of Mississippi delta coastal geomorphology using high resolution Multispectral Atmospheric Mapping Sensor (MAMS) data". In *5th Australasian Remote Sensing Conference*, Perth, Australia, pp. 738-745, 1990.

Guzzi, R., R. Rizzi, and G. Zibordi, "Atmospheric correction of data.measured by a flying platform over the sea: Elements of a model and its experimental validation". *Applied Optics*, Vol. 26, pp. 3043-3051, 1987.

Huh, O. K., H. H. Roberts, L. J. Rouse, and D. L. Rickman, "Fine grain sediment transport and deposition in the Atchafalaya and Chenier Plain sedimentary system". In *Coastal Sediments '91: Proceedings of Specialty Conference*, American Society of Civil Engineers, Seattle, WA, pp. 817-830, 25-27 June 1991.

Kuo, N. J., and X. H. Yan, "Using the shape-matching method to compute sea-surface velocities from AVHRR satellite". *IEEE Trans. Geosci. Remote Sens.*, Vol. 32, No. 3, pp. 724-728, May 1994.

Moeller, C. C., O. K. Huh, H. H. Roberts, L. E. Gumley, and W. P. Menzel, "Response of Louisiana coastal environments to a cold front passage". *J. Coastal Res.*, Vol. 9, No. 2, pp. 434-447, 1993.

Moeller, C. C., W. P. Menzel, and O. K. Huh, "A look at the use of GOES-8 data for monitoring water motions in turbid coastal waters". In *Eighth Conference on Satellite*

Meteorology and Oceanography, American Meteorological Society, Atlanta, GA, pp. 435-438, Jan 28 - Feb. 2, 1996.

Roberts, H. H., O. K. Huh, S. A. Hsu, L. J. Rouse, Jr., and D. Rickman, "Impact of cold-front passages on geomorphic evolution and sediment dynamics of the complex Louisiana coast". In *Coastal Sediments '87: Proceedings of Specialty Conference*, American Society of Civil Engineers, New Orleans, LA, pp. 1950-1963, May 12-14, 1987.

N. D. Walker, L. J. Rouse, jr, O. K. Huh, D. E. Wilensky, and V. Ransibrahmanakul, "Assessing the spatial characteristics and temporal variabilities of the Mississippi and Atchafalaya River plumes". In *Proceedings, First Thematic Conference on Remote Sensing for Marine and Coastal Environments*, ERIM, New Orleans, LA, pp. 719-728, June 1992.

COASTAL ZONE APPLICATIONS OF MODES FROM AIRCRAFT AND SATELLITE

Christopher C. Moeller[1], Oscar K. Huh[2], W. Paul Menzel[3]

[1]Cooperative Institute for Meteorological Satellite Studies; University of Wisconsin
[3]NOAA/NESDIS/ASPP
1225 West Dayton Street
Madison, WI 53706-1695

[2]Coastal Studies Institute; Louisiana State University
308 Howe-Russell Geoscience Complex
Baton Rouge, LA 70803-7527

1.0 INTRODUCTION

The MODerate resolution Imaging Spectrometer (MODIS) is scheduled for launch into polar orbit in summer 1998. MODIS has 36 channels in the visible and infrared region at various spatial resolutions of 250, 500, and 1000 meters. MODIS, as part of the Earth Observing System (EOS), will provide data for generation of atmospheric (e.g. cloud properties, aerosols), oceanic (e.g. ocean productivity, sea surface temperature) and land surface (e.g. land surface temperature, vegetation index) products. Applications of MODIS data to coastal studies merit further study. The MODIS 250 meter resolution visible channels will provide a high resolution map of coastal environments on a repeat cycle similar to current AVHRR monitoring.

TABLE 1. Spectral characteristics of the 50-channel MODIS Airborne Simulator (MAS),

* indicates equivalent MODIS channel.

MAS channel	Central wavelength (μm)	Spectral resolution (μm)	MAS channel	Central wavelength (μm)	Spectral resolution (μm)	MAS channel	Central wavelength (μm)	Spectral resolution (μm)
1*	0.547	0.044	18	2.030	0.048	35	4.36	0.15
2*	0.657	0.053	19	2.080	0.047	36*	4.51	0.15
3	0.704	0.042	20*	2.129	0.047	37	4.66	0.16
4*	0.745	0.041	21	2.178	0.047	38	4.82	0.16
5	0.786	0.041	22	2.227	0.047	39	4.97	0.15
6	0.827	0.042	23	2.276	0.046	40	5.12	0.15
7*	0.869	0.042	24	2.327	0.047	41	5.28	0.16
8*	0.909	0.033	25	2.375	0.047	42*	8.59	0.44
9*	0.947	0.046	26	2.96	0.16	43*	9.77	0.62
10*	1.609	0.052	27	3.11	0.16	44	10.54	0.49
11	1.663	0.052	28	3.27	0.16	45*	11.01	0.54
12	1.723	0.050	29	3.42	0.17	46*	11.97	0.45
13	1.775	0.049	30	3.58	0.16	47	12.85	0.46
14	1.825	0.046	31*	3.74	0.16	48*	13.24	0.48
15	1.879	0.045	32*	3.90	0.16	49*	13.71	0.60
16	1.932	0.045	33*	4.05	0.15	50*	14.19	0.42
17	1.979	0.048	34	4.21	0.16			

The MODIS Airborne Simulator (MAS) (King et al.,1996) was developed as an airborne simulator for the MODIS instrument. MAS contains visible and infrared bands that will be available from MODIS (Table 1). On NASA's ER-2 platform (nominal 20 km altitude), MAS collects 50 meter resolution data across a 37 km swath. Beginning in 1994, MAS has flown missions over Louisiana's Gulf coast, mapping suspended sediment transport, nearshore water temperature, coastal water types, and circulation patterns in response to cold front wind system forcing (Moeller et al.,1993). MAS (and MODIS) applications to coastal hazards (e.g. oil spill, storm impact) are the topic of this discussion.

2.0 MAS APPLICATIONS

2.1 MAS WATER MOTION DETECTION

On the aircraft platform, MAS is capable of tracking inwater features (e.g. turbidity, pollutants, watercraft) in coastal waters through repeated mapping of flight lines over short time intervals (hours). This approach has been used for tracking sediment transport in nearshore coastal waters (Mueller et al.,1996), an example of which is shown in Figure 1. In Figure 1,

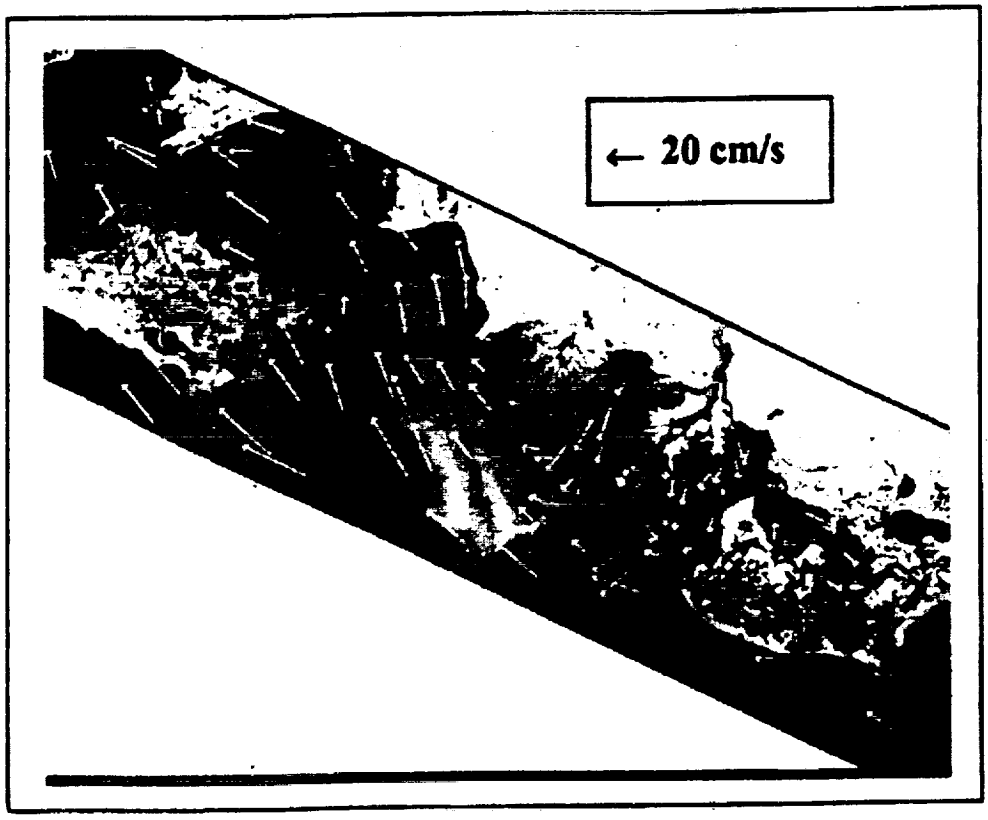

Figure 1. Water Motion Velocity Estimates from MAS 24 January 1995 Data.

turbidity contrast made it possible to subjectively select and track features for water motion estimation. Accurately georeferencing the MAS data is critical, as displacements of recognizable water features are typically small over the three to six hours that the ER-2 aircraft can spend monitoring a given location (note: the development of Unmanned Aerospace Vehicles (UAV) can significantly extend onsite duration). The presence of land features in the data of Figure 1 facilitates good georeferencing of the data; GPS systems on aircraft help for water-only scenes. MAS water motion vectors provide a picture of the circulation responsible for near-surface transport of inwater material.

One possible application, directly tracking oil slick features, has not been attempted with MAS data although oil slicks have been detected in visible spectral data when sunglint is present. This approach limits direct oil slick detection to daytime conditions. Spectral signatures of oil (and other pollutants) need to be identified for nighttime detection. A combined MAS and Synthetic Aperture Radar (SAR) data set should be collected to explore synergism between these data types for surfactant detection. Knowledge gained from such a data set would likely be directly applicable to MODIS data.

2.2 MAS WATER TYPE DISCRIMINATION

Analyses of MAS visible, near infrared (NIR) and longwave infrared (LWIR) data have shown that the various water sources, or types, present in the coastal environment can be discriminated from one another using multispectral analysis. Diagrams of turbidity versus water temperature separate water types. This tool has been demonstrated using MAS data along the Louisiana coast (Huh et al., 1996). Turbidity estimates are taken from MAS visible/NIR atmospherically corrected data; sea surface temperature estimates are made using a split window technique with MAS 11 and 12 micron data. Investigations have shown that a myriad of water types (saline Gulf, river, fresh marsh, soil drainage from sub-aerially exposed deltaic sand banks, bay, and salt marsh) are present after a cold front passage, due to local surface winds driving down water levels in the coastal environment. The presence of these water types is a signal of ongoing vitality of these specialized environments, especially in the wake of damaging tropical systems.

Land surface types can also be discriminated using multispectral analysis. It is anticipated that marsh, bare soil/sand, vegetated, burned, etc. regions are identifiable using MAS data. Such analyses bring additional information to storm impact assessment, including overwash, marsh destruction, vegetation and agricultural destruction. Large (hundreds of meters) changes in coastal landform (erosion and deposition) are also identifiable with MAS data.

2.3 COASTAL LANDFORM IMPACT

The Louisiana coast is experiencing gradual but continuous subsidence (from 1.5 to 5 cm/ yr) of its landform. Without continued influx of sediment from the Mississippi River distributary system, coastal landform eventually subsides below sea level and is flooded. The end result is salt

water encroachment and destruction of coastal freshwater environments. Petroleum industry interests in the coastal zone require access channeling which further reduces sediment dispersal into freshwater marsh environments. Recently, a plan has been enacted to improve sediment dispersal along the coast by opening crevasses (breeches in the levee). Monitoring sediment dispersal around crevasses is valuable for understanding the efficacy of this management approach. MAS has the high spatial resolution and multispectral capability to contribute to the assessment. The impact of tropical storms on crevasses must also be monitored. The disabling or destruction of crevasses limits sediment dispersal and effectively accelerates landloss. MAS water motion estimation provides a dynamic assessment of sediment dispersal in and around crevasses.

3.0 DISCUSSION AND SUMMARY

Coastal environments are among the most sensitive of the Earth system. Because of their ability to support a wide variety of marine and terrestrial life, they are also among the most vital. Management strategies which support fragile coastal ecosystems and yet maintain fisheries, petroleum, recreational, and human habitation interests require detailed knowledge of natural and anthropogenic impacts on these environments. These impacts include surfactant discharge, tropical and extra-tropical storm impact, and man-induced landform change, among others.

As part of an ongoing effort, data from the MODIS Airborne Simulator (MAS) has been used to monitor the Louisiana coastal environment, primarily for suspended sediment dispersal and water type identification. From NASA's ER-2 platform, MAS 50m resolution data can be collected over 3 to 6 hour periods for monitoring coastal environments with visible, near infrared and thermal infrared spectral data. Applications developed for MAS data will be transferred to NASA's MODerate resolution Imaging Spectrometer (MODIS) scheduled for launch into polar orbit in summer 1998 (AM platform). MODIS, as part of the Earth Observing System (EOS), will play a prominent role in the Earth system science of the Mission To Planet Earth (MTPE) program.

MAS should be viewed as a tool for monitoring water motions and transport during events which require knowledge of transport for planning remedial action (such as oil spills). MAS is also a tool for assessing impact on coastal environments by storm systems through identifying water types and landform change. As a visible/infrared spectrometer, MAS measurements are affected by clouds. Coupling MAS with SAR imagery should provide an enhanced description of coastal zone conditions. Use of SAR technology to characterize wave conditions during storms may provide an important link between atmospheric forcing and sea state response.

REFERENCES

Huh, O. K., C. C. Moeller, W. P. Menzel, L. J. Rouse, Jr. and H. H. Roberts, 1996: Remote sensing of turbid coastal and estuarine water: A method of multispectral water-type analysis. Accepted for publication in Jour. Coastal Res., 12 (4).

King, M. D., W. P. Menzel, P. S. Grant, J. S. Myers, G. T. Arnold, S. Platnick, L. E. Gumley, S. Tsay, C. C. Moeller, M. Fitzgerald, K. S. Brown, and F. Osterwisch, 1996: Airborne scanning spectrometer for remote sensing of cloud, aerosol, water vapor and surface properties. J. Atmos. and Oceanic Technol., 13, 777-794.

Moeller, C. C., O. K. Huh, H. H. Roberts, L. E. Gumley, and W. P. Menzel, "Response of Louisiana coastal environments to a cold front passage". J. Coastal Res., Vol. 9, No. 2, pp. 434447, 1993.

Moeller, C. C., O. K. Huh, W. P. Menzel, and H. H. Roberts, 1996: The use of aircraft-borne MAS data for mapping sediment transport along the Louisiana coast. Second International Airborne Remote Sensing Conference and Exhibition, San Francisco, CA. 24-27 June, 1996, ERIM, Vol. II, pp 673-682.